A graptolite-rich Ordovician–Silurian boundary section in the south-central Pyrenees, Spain: stratigraphical and palaeobiogeographical significance

PETR ŠTORCH[1], JOSEP ROQUÉ BERNAL[2] & JUAN CARLOS GUTIÉRREZ-MARCO[3]

[1] *Institute of Geology of the Czech Academy of Sciences, Rozvojová 269, 165 00, Praha 6, Czech Republic* [*storch@gli.cas.cz*]

[2] *Sant Benilde 8, 2º 1ª, 43006 Tarragona, Spain.*

[3] *Instituto de Geociencias (CSIC, UCM), Dr. Severo Ochoa 7 planta 4, 28040 Madrid, and Departamento de Geodinámica, Estratigrafía y Paleontología, Facultad CC. Geológicas UCM, José Antonio Novais 12, 28040 Madrid, Spain.*

Abstract: An Ordovician–Silurian boundary section marked by an uninterrupted, relatively high rate of black-shale sedimentation and abundant, diverse graptolites is described from the south-central Pyrenees. The structurally simple Estana section comprises the uppermost part of the quartzite-dominated Bar Formation and overlying black shales of late Hirnantian and early Rhuddanian age which have been dated by graptolites to the upper *Metabolograptus persculptus* and lower–middle *Akidograptus ascensus–Parakidograptus acuminatus* biozones. Due to the absence of *M. persculptus*, a *Metabolograptus parvulus* Biozone correlative with the upper part of the *persculptus* Biozone is recognized below the lowest occurrence of akidograptids which indicate the base of the Silurian System. The graptolite fauna comprises 27 species including *Normalograptus minor*, *N. lubricus*, *N. rhizinus*, *Hirsutograptus*, *Korenograptus bifurcus*, *K. bicaudatus, K. lanpherei* and *Nd. shanchongensis*, most of which were formerly considered to be endemic to the low-latitude palaeobiogeographical province of China, Siberia and northern North America. Two new species, *Normalograptus baridaensis* and *N. ednae*, are described. The succession of graptolite assemblages in the Estana section and occurrence of several cosmopolitan taxa in its *parvulus* and lower *ascensus–acuminatus* biozones that are unknown elsewhere in peri-Gondwanan Europe suggest that strata immediately surrounding the O–S boundary may be absent, highly

condensed, or oxic and barren of graptolites in other sections of north-western peri-Gondwana. Common graptolite synrhabdosomes and abnormal rhabdosomes may indicate some environmental stress in the *parvulus* Biozone, although the rather uniform black shale lithology, TOC content and $\delta^{13}C_{org}$ values suggest uninterrupted sedimentation under stable, anoxic conditions.

Key words: Ordovician–Silurian boundary, graptolites, biostratigraphy, black shale, carbon isotopes, synrhabdosome, abnormal astogeny

1. Introduction

The Ordovician–Silurian boundary interval was a remarkable period of climatic, environmental and sea-level changes. Rapid deglaciation of the Earth's southern hemisphere brought a dramatic rise in global sea-level, weakened oceanic circulation and enhanced stratification of water masses. Profound environmental changes are documented by faunal and sedimentary turnover associated with conspicuous geochemical signatures. The Ordovician–Silurian boundary is marked by an anoxic event recorded world-wide (Melchin *et al*. 2013). In the majority of European sections postglacial upper Hirnantian mudstones and shales, occasionally with the trilobite *Mucronaspis* and *Hirnantia* shelly brachiopod fauna, are sharply overlain by anoxic black shales with abundant graptolites. This scheme, however, varies depending on the palaeogeography and location relative to the shoreline and the local rate of sedimentation. In the offshore successions of Baltica, represented by sections and drill cores in Bornholm (Bjerreskov, 1975; Koren' & Bjerreskov, 1997) and southern Sweden (Bergström *et al*. 1999; Koren', Ahlberg & Nielsen, 2003), the lowermost part of the black shale succession has yielded low-diversity to moderately diverse graptolite faunas of the upper Hirnantian *Metabolograptus persculptus* Biozone. Graptolites of the *persculptus* Biozone have been reported also from north-eastern Poland (Masiak, Podhałańska & Stempień-Sałek, 2003; Podhałańska, 2003; Trela *et al*. 2016). In the Avalonian Welsh Basin, the uppermost Ordovician strata contain several thin levels (Blackett *et al*. 2009) of black shale or mudstone with abundant *Metabolograptus persculptus* (Elles & Wood, 1907) and *Metabolograptus parvulus* (Lapworth, 1900). Moderately diverse graptolite assemblages from the *persculptus* Biozone, including the earliest monograptid *Atavograptus ceryx* (Rickards & Hutt, 1970), have been described from the Lake District, northern England (Rickards, 1970; Hutt, 1974). At the GSSP for the base of the Silurian System in Dob's Linn, southern Scotland (Williams, 1983; Melchin, 2003; Fan, Melchin & Williams, 2005), continuous black shale sedimentation commenced in the *persculptus* Biozone. The graptolite assemblage recorded by Fan, Melchin & Williams (2005) in the lowermost part of this black shale succession included several species [*Normalograptus minor* (Huang, 1982), *Normalograptus mirnyensis* (Obut & Sobolevskaya, 1967), *Normalograptus praetamariscus* (Li, 1984), *Normalograptus rhizinus* (Li & Yang, 1983), *Korenograptus laciniosus* (Churkin & Carter, 1970), *Normalograptus skeliphrus* (Koren' & Melchin, 2000), *Normalograptus ugurensis* (Koren' & Melchin, 2000) and *Neodiplograptus shanchongensis* (Li, 1984)] previously

recognized in the low-latitude palaeobiogeographical province of China, Central Asia, Siberia and northern North America outlined by Melchin (1989).

In peri-Gondwanan Europe, the graptolite record across the Ordovician–Silurian boundary is rather different, less abundant and less complete. *Metabolograptus persculptus*, locally accompanied by tentatively determined normalograptid rhabdosomes, *Mucronaspis* trilobites and *Hirnantia* brachiopod faunas, has been collected from Hirnantian mudstones of the Prague Synform in the Czech Republic (Nová Ves, Pankrác, Praha-Nové Butovice and Praha-Řepy sections; Štorch, 1986; Štorch & Loydell, 1996), from Saxony (Frankenberg section; Jaeger, 1977), the Austrian Southern Alps (Cellon and Feistritsgraben sections; Jaeger, Havlíček & Schönlaub, 1975; Štorch & Schönlaub, 2012) and western Bulgaria (Sachanski, 1993; Lakova & Sachanski, 2004). Hirnantian graptolites are either missing (most sections in the Czech Republic, Thuringia, Sardinia, Brittany, Nontagne Noire, Portugal and Spain), badly preserved (Bulgaria, Austrian Carnic Alps), confined to a distinct level separated by a barren interval from the basal Silurian *ascensus* Biozone (Řepy, Nové Butovice, Nová Ves and Běchovice sections in the Czech Republic, Frankenberg section in Saxony), or both. Lowermost samples of the Silurian black shales exhibit rich graptolite faunas dominated by *Akidograptus ascensus* Davies, 1929, *Neodiplograptus lanceolatus* Štorch & Serpagli, 1993 and normalograptids in all coeval sections from Portugal (Piçarra *et al*. 1995) and Spain (Jaeger & Robardet, 1979; Gutiérrez-Marco & Robardet, 1991; Roqué, 1999), through Brittany (Piçarra *et al*. 2009), Montagne Noire (Štorch & Feist, 2008), Sardinia (Štorch & Serpagli, 1993), Thuringia and Saxony (Schauer, 1971), northern Bavaria (Stein, 1965), central Bohemia (Štorch, 1996), and eastern Serbia (Krstič, Maslarevič & Sudar, 2005) to western Bulgaria (Lakova & Sachanski, 2004). The biostratigraphy and graptolite assemblages of the *Akidograptus ascensus–Parakidograptus acuminatus* Biozone of peri-Gondwanan Europe were reviewed by Štorch (1996). A rather different assemblage, including exotic graptolite species, was described by Štorch & Schönlaub (2012) from the Waterfall Section near Zollnersee in the Austrian Southern Alps. Undeterminable normalograptids occur throughout much of the latter black, cherty succession, while determinable specimens including *Parakidograptus* 'acuminatus' (Nicholson, 1867) and *Korenograptus bifurcus* (Mu *et al.*, 1974) [= *Rickardsograptus bifurcus* (Ye, 1978)] are confined to a rather thin interval 92–102 cm above the top of the thick uppermost bed of quartzite. Some doubts about the high-resolution biostratigraphy of the O–S boundary faunas of Europe, and about biostratigraphical and palaeobiogeographical interpretations of the Austrian fauna in particular, can be resolved owing to the recent discovery of the richly fossiliferous Ordovician–Silurian boundary section near Estana village in the south-central Pyrenees of Spain (Fig. 1). A preliminary report on the Estana section was presented to the Geological Society of Spain by Roqué Bernal, Štorch & Gutiérrez-Marco (2017), who identified six graptolite species and provided an approximate placement of the O–S boundary above the Bar Quartzite. Further study of the section and graptolite material has revealed that the *M. persculptus* of the latter authors belongs in *M. parvulus* which is a closely similar species, common in the upper *persculptus* Biozone and uncommon in the *ascensus–acuminatus*

Biozone. Stratigraphically highest records came from Jordan, from strata tentatively refered to lower *Cystograptus vesiculosus* Biozone by Loydell (2007).

The Estana section, discovered by JRB and described in detail in this paper (Fig. 2), is unique in a European context in having uniform, uninterrupted and adequately rapid black shale sedimentation across the Ordovician–Silurian boundary interval, combined with a rich, continuous and moderately well-preserved graptolite fossil record. Sedimentation rate is comparable with those in deep-water black-shale O–S boundary sections in Dob's Linn, Scotland (Williams, 1983) or Röstanga core in Southern Sweden (Koren' *et al.* 2003). Black shales overlying the quartzites of the Bar Formation contain a high-diversity graptolite fauna with two new and several age-diagnostic taxa along with the biostratigraphical marker species *M. parvulus* and cosmopolitan biozonal-indices *A. ascensus* and *Par. acuminatus*.

2. Methods and materials

The section, repeatedly studied by the authors since 2013, was systematically sampled for its graptolite fossil record, lithologies and organic carbon geochemistry. Each 20 cm thick interval of the section was studied bed-by-bed and graptolites were collected from a rock volume of *c.* 0.03 m^3 per sample. Some intervals were divided into two 10 cm thick parts and resampled. Graptolites are preserved as flattened impressions with periderm partly pyritized and for the most part covered by pale mineral overgrowths that make rhabdosomes clearly visible against the black shale. Common preservation of long nemata, long and complex virgellar structures as well as complete synrhabdosomes indicates a quiet depositional environment without significant post-mortem transport. Bedding planes covered by aligned rhabdosomes are rare. The effects of tectonic strain have changed proportions and measured parameters of some specimens by 5–10 %. Illustrated and measured specimens are housed in the Museo Geominero, Instituto Geológico y Minero de España, Madrid and bear an MGM designation.

The section was sampled for total organic carbon content (TOC) and organic carbon isotope composition at the same regular intervals (20 cm and 10 cm) from the base of the black shale succession to the top of the measured section. Hand specimens were cut and rock powder was prepared from a few grams of a fresh sample. A few milligrams of rock powder were taken for TOC and isotope analyses. Before analyses, rock powders were decarbonatized, then washed and dried. Total organic carbon content was analysed in the Geological Institute AS CR, Prague. Carbon isotope analyses were performed by GeoZentrum Nordbayern, Erlangen, with a Flash EA 2000 elemental analyser connected online to ThermoFinnigan Delta V Plus mass spectrometer. Carbon isotope values are related to V-PDB. Accuracy and reproducibility of the analyses were checked by replicate analyses of laboratory standard CH_4N_2O calibrated to international standards USGS 40 and 41. Reproducibility was better than ±0.1‰ (1σ).

3. Geological setting

The studied section is located on the southern edge of the central Pyrenees Axial Zone, west of the La Cerdanya Neogene basin (Fig. 1). It is exposed adjacent to the old mountain track from Estana to Querforadat, on the left (southern) bank of the Segre River valley in the province of Lleida, NE Spain. The main graptolite-bearing section is within an isolated outcrop of uppermost Ordovician sandstones and lowermost Silurian black shales surrounded by weathered Carboniferous–Permian dacitic lavas and Holocene sediments. The locality lies on the hill-slope above the right bank of the Riu del Quer (= Quer stream), *c*. 1,200 m southwest of the village of Estana, and 400 m south of fossil locality nº 68 of Dégardin (1988, fig. 203), from where this author listed 19 Aeronian graptolite species. Geographical coordinates for the base of the Silurian (base of the *ascensus–acuminatus* Biozone) in the Estana section are 42º 18′ 51.65″ N and 1º 39′ 2.68″ W.

The highest Ordovician succession in the the central Pyrenees is very similar to those of the Canigó Massif in the axial part of the eastern Pyrenees. In both areas, above calcareous shales and limestones of the Estana Formation (up to 150 m thick) with Kralodvorian (late Katian–Ka3-4) brachiopods and conodonts (Hartevelt, 1970; Gil-Peña *et al.* 2004; Colmenar, 2015), there are poorly bedded dark slates of the Ansovell Formation (20–300 m thick), followed by the Bar Quartzite (0–20 m of dark-grey, medium-grained sandstone) which is overlain by black shales with graptolites. The supposed record of Late Ordovician brachiopods near the base of the Bar Quartzite (Hartevelt, 1970), and of middle Rhuddanian to Aeronian graptolites in the overlying black shales (Roussel, 1904; Dalloni, 1930; Boissevain, 1934; Dégardin, 1988, 1990), has led to different interpretations about the placement of the Ordovician–Silurian boundary. For some authors it should be at the base of the quartzite unit (Schmidt, 1931; Boissevain, 1934), for others at the top (Hartevelt, 1970; Dégardin *et al.* 1996; Casas, 2010) or at an undetermined level within this unit (Gil-Peña *et al*. 2001, 2004; Gil-Peña & Barnolas, 2007; Puddu & Casas, 2011; Casas & Palacios, 2012; Margalef *et al.* 2016; Casas, Puddu & Álvaro, 2017; Puddu, Casas & Álvaro, 2017). Brachiopods found by Hartevelt (1970) in the Bar Quartzite and reviewed by E. Villas (in Gil-Peña *et al.* 2004) represent reworked specimens derived from both the Estana and Cava formations, the latter of late Berounian (*c.* Ka2) age. Gil-Peña *et al.* (2001) referred to an important erosive unconformity at the top of the Ansovell Formation, probably related to the sea-level fall resulting from the Hirnantian glaciation, which is locally overlain by a discontinuous conglomerate containing pebbles of some older Upper Ordovician stratigraphic units. The Bar Quartzite, overlying the paleorelief infilled by conglomerates or the Ansovell Formation, is interpreted as a transgressive unit attributed to the sea-level rise at the end of the glacial event. Recent dating of detrital zircons from the Bar Quartzite of the Rabassa dome (Pyrenean Axial Zone: Margalef *et al.* 2016) yielded a youngest peak age of 443 Ma, thus close to the Ordovician–Silurian boundary estimated at 443.8 ± 1.5 Ma according to the latest edition (2017/02) of the International Chronostratigraphic Chart. Detrital zircons from Ordovician sediments of Pyrenees and SW Sardinia studied by Margalef *et al*. (2016) indicate that the two terranes shared the same source area. Both terranes were situated near the northern Gondwana margin, in front of Arabian-Nubian Shield between Arabian-Nubian drainage system in the East and present day Libya and Algeria in the West.

The discovery of the new, complete and richly fossiliferous Estana section has revealed the true position of the Ordovician–Silurian boundary in the south-central Pyrenees (Roqué Bernal, Štorch & Gutiérrez-Marco, 2017). In the Riu de Quer area (Estana section), the Bar Quartzite shows a sharp and well defined upper conformable contact with the black graptolitic shales that have been unanimously considered to be Silurian by all preceeding authors. Our study extends over the first 4.1 m of the unnamed formation known in the literature as the 'lower graptolitic shales', 'black shales with graptolites' or 'black graphitic shales'. In these strata we found a specific graptolite assemblage with abundant occurrence of *M. parvulus* and other taxa indicating the upper Hirnantian *persculptus* Biozone. The uninterrupted black shale succession continued into the lower Rhuddanian *ascensus–acuminatus* Biozone (Fig. 2). The Ordovician–Silurian boundary, marked by the First Appearance Datum of *A. ascensus*, is located 2.2 m above the top of the Bar Quartzite.

4. Graptolite record, biostratigraphy and correlation

Silty-micaceous black shales conformably overlying the thin-bedded quartzites of the Bar Formation are rich in relatively diverse graptolites (Fig. 3) tentatively assigned to the upper part of the *persculptus* Biozone. True *M. persculptus* is missing in the Estana section but the closely related *M. parvulus*, which is a common species of the upper *persculptus* Biozone (see Melchin, McCracken & Oliff, 1991; Loydell *et al*. 2002; Blackett *et al*. 2009), is abundant in association with *Normalograptus ajjeri* (Legrand, 1977), *N. minor*, *Normalograptus angustus* (Perner, 1895) and *Normalograptus baridaensis* sp. nov. The *parvulus* Biozone correlatable with the upper part of the *persculptus* Biozone is defined in the section as the interval between FAD of *M. parvulus* and FAD of *A. ascensus*.

Normalograptus minor was first described from the uppermost Hirnantian of Tibet, China and later recorded from the same level in the Yangtze region of China (Chen *et al*., 2005) and from the Dob's Linn GSSP section in Scotland (Fan, Melchin & Williams, 2005). Koren', Ahlberg & Nielsen (2003) reported *N. minor* from their pre-*ascensus avitus* Fauna of southern Sweden. A single specimen from the lower *ascensus–acuminatus* Biozone of south-western Sardinia, reported as *Normalograptus* sp. B by Štorch & Serpagli (1993), extends its range into the lowermost Rhuddanian.The species is particularly common 0.7–1.0 m above the top of the sandstone unit. Species richness further increased in the middle part of the local range of *M. parvulus*. *Normalograptus minor* disappears 1.9 m above the quartzite while *Normalograptus lubricus* (Chen & Lin, 1978), *Normalograptus* aff. *rhizinus* (Li & Yang, 1983) and *Glyptograptus dufkai* Štorch, 1992 joined the assemblage. Higher up the section, *N. ajjeri* becomes abundant whereas most other taxa made their last occurrences. Synrhabdosomes of *M. parvulus* (Fig. 4a) are common, along with a few synrhabdosomes of *N. ajjeri*, at several levels from 0.3 to 1.9 m above the base of the black shale succession (Fig. 2). Relatively common uniserial abnormalities in the astogenetic development of biserial rhabdosomes (Fig. 4b–e) suggest some environmental stress and/or phylogenetic experimentation.

Normalograptus lubricus was reported by Chen & Lin (1978) from a combined *ascensus–bicaudatus* Biozone of northern Guizhou Province, China in association with *A. ascensus*. Also *Climacograptus* sp. (cf. *Cl. miserabilis*) figured by Williams (1983) from the lower *acuminatus* Biozone (= *ascensus–acuminatus* Biozone as used herein) of Dob's Linn, Scotland belongs to *N. lubricus*. In Arctic Canada Melchin, McCracken & Oliff (1991) distinguished a specific *madernii–lubricus* Subzone in the lower part of the *acuminatus* Biozone despite the absence of akidograptid graptolites in this lower subzone. In Uzbekistan Koren' & Melchin (2000) recognized a *N. lubricus* Subzone in the lower part of their *ascensus* Biozone, again below the lowest occurrence of *A. ascensus*. In Saudi Arabia, Williams *et al.* (2016) recorded *N. lubricus* in association with *N. parvulus* and *Normalograptus bifurcatus* Loydell, 2007 in a distinct *lubricus* Biozone recognized by them below the lowest akidograptid occurrences. It is obvious that, in some regions at least, the appearance of *N. lubricus* preceded the formal base of the *ascensus* Biozone defined by the FAD of the nominal taxon. Thus, in a strict biostratigraphical sense, *N. lubricus* occurs in the uppermost Hirnantian in the Estana section, 0.3–1.0 m below the lowest *A. ascensus* and below the FADs of *K. bifurcus* and *N. rhizinus.* Graptolite fauna of the lower part of the Estana section can be recognized as a distinct, presumably time-specific assemblage (Fig. 5, Assemblage 2) tentatively correlated with upper *persculptus* Biozone assemblage in Scotland (Dob's Linn) and *avitus* Fauna reported by Koren', Ahlberg & Nielsen (2003) from the interval between the highest *M. persculptus* and lowest *A. ascensus* in southern Sweden (Röstanga core). The Assemblage 2 (see Fig. 6 for details) comprises four cosmopolitan species, *N. minor* thought to be confined in a low-latitude realm, *N. dufkai* of north-Gondwanan distribution and two 'local species' recorded first time. It has not been found in the O–S boundary sections elsewhere in peri-Gondwanan Europe.

Normalograptus rhizinus with its gradually tapering rhabdosome and long virgella widening into a small distal vane, *K. bifurcus* having a robust bifurcating virgella, and the lowest *N. mirnyensis* appeared in an about 0.3 m thick interval (Fig. 2, Samples EST 10, 10a, 10b, and 11a) between the last *M. parvulus* and first *A. ascensus.* The morphologically and stratigraphically significant *N. rhizinus* and *K. bifurcus* do not occur in the *avitus* Fauna of Koren', Ahlberg & Nielsen (2003). Records of *N. rhizinus* have been confined to the upper *persculptus* Biozone in both China (Chen *et al.* 2005) and Scotland (Fan, Melchin & Williams, 2005). *Korenograptus bifurcus* which is common in the lowermost Silurian of Sichuan Province, China, was reported by Štorch & Schönlaub (2012) from the *ascensus–acuminatus* Biozone of the Waterfall Section in the Austrian Southern Alps.

The base of the Silurian System is marked in the Estana Section by the lowest occurrence of *A. ascensus* 2.2 m above the top of the sandstone unit (Fig. 2, Sample EST 11b). It coincides, almost precisely, with the stratigraphically lowest *Parakidograptus praematurus* (Davies, 1929) and *Nd. shanchongensis*. The species richness of the graptolite fauna considerably increased as illustrated by Figures 7 and 8. The black shale is markedly less silty at this level than in the *parvulus* Biozone. A new assemblage (Figs. 5 and 6, Assemblage 3) comprised cosmopolitan *A. ascensus*, *Par. praematurus*, early *Par. acuminatus*, *Nd. shanchongensis*, *N. mirnyensis* and some other, long-ranging normalograptids along with four species widespread

in low-latitude palaeoplates of Asia and North America [*Korenograptus bicaudatus* (Chen & Lin, 1978), *Korenograptus lanpherei* (Churkin & Carter, 1970), *K. bifurcus* and *N. rhizinus*] and newly decribed *Normalograptus ednae* sp. nov. Peri-gondwanan elements represent *Gl. dufkai* and *Normalograptus crassus* Štorch & Feist, 2008. This assemblage is similar to that described by Štorch & Schönlaub (2012) from Austria in having *K. bifurcus* together with *Par. praematurus* identified as *Par. acuminatus* in that paper, early forms of *Par. acuminatus*, *N. ajjeri* and some *Glyptograptus. Neodiplograptus lanceolatus* and cosmopolitan *Normalograptus trifilis* (Manck, 1923) are absent in both the Austrian section and in the lower part of the *ascensus–acuminatus* Biozone in the Estana section. The joint occurrence of *K. bicaudatus* and *A. ascensus* allows for correlation of this level with the lowermost Silurian *ascensus–bicaudatus* Biozone defined in China by Chen & Lin (1978).

About 3 m above the base of the black shale succession (Fig. 2, 2.7–3.5 m, samples EST 14– EST 17) the graptolite fauna further diversified. *Parakidograptus praematurus* was gradually replaced by an early morphotype of *Par. acuminatus* distinguished from *Par. praematurus* by its later point of origin of th l¹, generally more protracted proximal part of the rhabdosome and more acuminate metathecae with triangular outline and flowing genicula. *Korenograptus bifurcus* with its substantial forked virgella is replaced by *K. lanpherei* with its simple, long and thinner virgella. This interval, which is dominated by abundant *N. ajjeri* and characterized by *N. crassus* and apparently short-ranging *N. ednae* sp. nov. with its short and robust triple basal spines (virgella and two lateral spines), incorporates also the highest occurrences of *Gl. dufkai*, *N. rhizinus*, *N. mirnyensis* and *Nd. shanchongensis*, rare *Metabolograptus*? aff. *parvulus* (Lapworth, 1900) and single specimens of *Normalograptus medius* (Törnquist, 1897) and *Rickardsograptus* sp.

A graptolite assemblage dominated by *Nd. lanceolatus* and *A. ascensus* associated with *N. trifilis*, *N. ajjeri*, *N. angustus*, *Cystograptus ancestralis* Štorch, 1985 and *Par. acuminatus* (Assemblage 4 in Figs 5 and 6) appears nearly 4 m above the base of the black shale succession in the Estana section (samples EST 18 – EST 20, Fig. 2). Early representatives of *Par. acuminatus* are difficult to distinguish from its ancestor *Par. praematurus* which made its lowest occurrence much lower, at about the same level as the earliest *A. ascensus*. The co-occurrence of the three species has led us to use the combined *ascensus–acuminatus* Biozone in the sense of Štorch (1996) rather than separate *ascensus* and *acuminatus* biozones. The *ascensus–acuminatus* Biozone is defined as the interval between the FAD of *A. ascensus* and the FAD of *Cystograptus vesiculosus* (Nicholson, 1868), the index species of the succeeding biozone which is also present in a higher part of the Estana section.

The graptolite assemblage from the uppermost samples of the Estana section has been reported from almost every graptolite-bearing Ordovician-Silurian boundary section of peri-Gondwanan Europe by Štorch (1996). It is typically found in the lower and lower-middle parts of the combined *ascensus–acuminatus* Biozone in other European and Spanish sections (Štorch, 1996) and recently recorded in Saudi Arabia (Williams *et al*. 2016). Faunal elements from Estana that are new to peri-Gondwanan Europe are few, but *K. bicaudatus*, *K. lanpherei* and *Hirsutograptus* sp. enhance correlation of this assemblage with the middle–upper

acuminatus Biozone or the middle–upper part of a combined *ascensus–acuminatus* Biozone in Asia and northern North America. *Korenograptus bicaudatus* has been employed as a lowermost Silurian zonal index taxon in the *ascensus–bicaudatus* Biozone in China (Chen & Lin, 1978), *K. lanpherei* is confined to the *acuminatus* Biozone in Alaska and northern Canada (Loxton, 2017) and *Hirsutograptus* Koren' & Rickards, 1996 is another taxon of particular biostratigraphical significance outside Europe. A *Hirsutograptus sinitzini* Subzone is distinguished in the upper part of the *acuminatus* Biozone in Arctic Canada (Melchin, McCracken & Oliff, 1991) and in the uppermost part of the *ascensus–acuminatus* Biozone in Uzbekistan (Koren' & Melchin, 2000) where its lowest occurrence coincides with the FAD of typical *Par. acuminatus*. Other hirsutograptids appear at the same stratigraphical level also in China (Chen *et al*. 2000), Tien Shan (Chaletskaya, 1960), Russian northern Siberia (Obut, Sobolevskaya & Nikolaev, 1967; Gogin *et al*. 1997) and the southern Urals of western Kazakhstan (Koren' & Rickards, 1996). Melchin (2001) identified *Hirsutograptus* in the middle *acuminatus* Biozone at Dob's Linn, southern Scotland.

5. TOC and organic carbon geochemistry

Little fluctuating and generally increasing TOC values,1.8–2.8 wt. % in the *parvulus* Biozone and 2.3–3.2 wt. % in the lower *ascensus–acuminatus* Biozone (Fig. 9) conform with the rather uniform black-shale lithology and may also indicate stable, slightly increasing palaeoproductivity and stable or slightly decreasing sedimentation rate. The interpreted relatively high rate of black shale sedimentation in the Estana section would have the potential to reveal short-term carbon isotope excursions across the Hirnantian–Rhuddanian (O–S) boundary interval much better than the more condensed, and possibly incomplete sedimentary record preserved in many other sections of peri-Gondwanan Europe. The $\delta^{13}C_{org}$ values, varying from -29.84 ‰ to -30.60 ‰ with a general shift to lower values (Fig. 8), are consistent with values and trends recorded from other fully anoxic O–S boundary sections (Underwood *et al*. 1997; Fan, Peng & Melchin, 2009; Melchin *et al*. 2013) and suggest that black shale sedimentation commenced in the Estana section well after the end of Hirnantian positive carbon isotope excursion (HICE), which is consistent with the biostratigraphical dating of the lowermost black shale samples to the upper part of the *persculptus* Biozone. Minor decline in the $\delta^{13}C_{org}$ values below the base of the *ascensus–acuminatus* Biozone (samples EST 8–11a) resembles minor negative excursion recorded in the same stratigraphic level at Dob's Linn (Underwood *et al*. 1997) and Wangjiawan (Fan *et al*. 2009) sections. However, significant negative correlation between TOC and $\delta^{13}C_{org}$ using three correlation coefficients (Pearson's r = -0.62, Spearman's r_s = -0.49 and Kendall's tau = -0.40) indicate partial post-diagenetic opening of the carbon isotope system, possibly related to Carboniferous–Permian dacitic lavas exposed nearby. The $\delta^{13}C_{org}$ data must be considered with reservation in the Estana section despite fairly normal values matching other coeval sections.

6. Discussion

The Ordovician–Silurian boundary strata exposed in the Estana section not only yield a diverse and unique graptolite fauna with several species previously unknown from Europe but also have revealed some deviations in stratigraphical occurrences of the graptolite taxa.

Since no *M. persculptus s.s.* has been found in the Estana section, the exact biostratigraphical correlation of Assemblage 2 (Fig. 5) recovered from the black-shale interval below the lowest occurrence of akidograptids is based upon the co-occurrence of other biostratigraphically useful species. The closely similar, but smaller *M. parvulus*, which is common in the uppermost part of the *persculptus* Biozone all around the world and continues into the *ascensus–acuminatus* Biozone in some sections (Loydell, 2007; Blackett *et al.* 2009), is abundant in the lower part of the Estana section. It is accompanied by both long-ranging normalograptids and *N. minor* which has been described from the upper Hirnantian part (*persculptus* Biozone) of the Lungmachi Formation (Yangtze Platform, China). *Normalograptus rhizinus*, which also occurs in the upper *persculptus* Biozone in China and southern Scotland, made its lowest occurrence two samples below the lowest occurrence of *A. ascensus* in the Estana section and ranges well into the lower part of the *ascensus–acuminatus* Biozone. *Normalograptus lubricus*, described by Chen & Lin (1978) from the lowermost *ascensus–bicaudatus* Biozone of China and recorded from the same level in southern Scotland (Fan, Melchin & Williams, 2005) and Arctic Canada (Melchin, McCraken & Oliff, 1991), gives its name to a subzone in Uzbekistan (Koren' & Melchin, 2000) and a biozone in Saudi Arabia (Williams *et al.* 2016). It is confined to the uppermost part of the newly established *parvulus* Biozone, still below the lowest occurrence of akidograptids. We suppose that at least the upper part of the *parvulus* Biozone, *c.* 1.1–2.2 m above the base of the black shale succession, can be correlated with the *lubricus* Biozone of Koren' & Melchin (2000) and Williams *et al.* (2016) as well as with the rather different graptolite fauna of the pre-*ascensus* interval recognized by Koren', Ahlberg & Nielsen (2003) in Sweden. Considering that this nearly cosmopolitan fauna has not yet been recorded in any other section in peri-Gondwanan Europe, we could speculate that such a unique graptolite assemblage spread under specific environmental conditions enabling immigration of distinct elements of low-latitude faunas (*sensu* Melchin, 1989) in the course of post-glacial climate amelioration and major rise of sea-level. Indeed, specific and unusual environmental conditions in the Ordovician, pre-*ascensus* part of the Estana section could be inferred from the abundant occurrence of graptolite synrhabdosomes [Fig. 4a, see also Gutiérrez-Marco & Lenz (1998) for discussion] and from abnormal astogeny with uniserial development in biserial taxa (*Metabolograptus* and *Normalograptus*, Fig. 4b–e). Such abnormalities had to be more widespread, although not ubiquitous in the O–S boundary interval as indicated by synrhabdosomes of *Normalograptus* ex gr. *normalis* and *M. persculptus* s.l. from the *persculptus* Biozone of Mauritania (Underwood, Deynoux & Ghienne, 1998) and uni-biserial rhabdosomes recorded in a notably similar interval at Dob's Linn, the O–S boundary GSSP (Williams, 1983, text-figs. 3b, 7d, 8h; Muir, 2011, fig. 1). It is worth to note that present

author (PŠ) recorded numerous synrhabdosomes of *Neodiplograptus africanus* (Legrand) in lower–middle Rhuddanian of Mauritania which indicates that synrhabdosomes were linked to regional environment rather than being entirely time-specific.

Mature septate biserial rhabdosomes split distally into two long uniserial stipes, each furnished with a nema, suggest that abnormal colonies were able to grow until full maturity typical of other specimens of the respective species. Specimens from the Estana section support Muir's (2011) assumption that fine-tuning of rhabdosome hydrodynamics was not essential for further growth and survival of the graptolite colony. Common uniserial growth in the distal part of biserial graptolite taxa due to post-mortem breakage during transport of the rhabdosomes suggested by Williams (1983) can be excluded in the Estana section because of the common co-occurrence of unbroken long and complex virgellar structures, nemata and complex synrhabdosomes.

The common occurrence of abnormal specimens in the uppermost Hirnantian black shales of the Estana section may be considered as evidence of stressful environmental conditions. Synrhabdosomes have been interpreted by Gutiérrez-Marco & Lenz (1998) as temporary structures perhaps formed in relatively restricted water masses with low food supply. Also 'teratological events' recognized by Delabroye *et al.* (2012), Munnecke *et al.* (2012) and Vandenbroucke *et al.* (2015) in other planktic groups near the Ordovician–Silurian boundary have been related to diverse causes that generated a high level of environmental stress such as upwelling of anoxic/dysoxic waters, heavy metal pollution, or acidification due to explosive volcanism. Better understanding of causal relations among environmental changes near the Ordovician–Silurian boundary and their biotic response will require further consideration since both abnormal graptolite colonies and synrhabdosomes appeared in the Estana section in the same stratigraphical interval that witnessed the incipient adaptive radiation of the graptolite faunas after the latest Katian–early Hirnantian mass extinction event, including the origination of the uniserial monograptid colony.

In the Estana section, the relatively low-diversity graptolite assemblage of the uppermost samples of the upper Hirnantian *parvulus* Biozone was succeeded by an assemblage comprising *N. rhizinus*, *N. mirnyensis*, *N. crassus*, *K. bicaudatus*, *K. bifurcus*, *K. lanpherei*, *Nd. shanchongensis*, *M.?* aff. *parvulus*, *A. ascensus, Par. praematurus* and long-ranging normalograptids, later joined by *N. ednae* and an early form of *Par. acuminatus*. This high-diversity assemblage, which is confined to the lower part of the *ascensus–acuminatus* Biozone in the Estana section (Figs. 5, 6; Assemblage 3), is unique in a European context, with the partial exception of the Austrian Southern Alps (having *K. bifurcus* and *Par. praematurus*), and of southern Scotland having *Par. praematurus*, *N. mirnyensis*, *N. rhizinus* and *Nd. shanchongensis*. A few elements of this assemblage associated with *Nd. lanceolatus* (Fig. 5, Assemblage 3a) ranged up to a slightly higher stratigraphical level in the *ascensus–acuminatus* Biozone. Species have been reported also from Montagne Noire [*N. crassus* – (Štorch & Feist, 2008)], Sardinia [*N. crassus*, determined as *N. medius* by Štorch & Serpagli (1993)], Bohemia [*G. dufkai* – (Štorch 1996)], Bulgaria [*Par. praematurus* – (Lakova &

Sachanski 2004)] and Saudi Arabia [*N. crassus* – determined as *N. medius* by Williams *et al.* (2016, fig. 11C)].

Abundant occurrences of *N. trifilis*, *Nd. lanceolatus*, *Cyst. ancestralis*, *A. ascensus* and *Par. acuminatus* in the uppermost part of the Estana succession (samples EST 18 – EST 20) belong to Assemblage 4 (Figs. 5, 6) which is known from the lower–middle part of the combined *ascensus–acuminatus* Biozone in the majority of lower Rhuddanian black shale sections in peri-Gondwanan Europe (see Štorch, 1996 and Štorch & Feist, 2008 for summary), north-eastern Morocco (PŠ, personal observation), Jordan (Loydell, 2007), Saudi Arabia (Williams *et al.* 2016), Scotland (Williams, 1983 and M.J. Melchin, pers. comm.), eastern Poland (Masiak *et al.* 2003) and southern Sweden (Koren' *et al.* 2003). In this interval, *Par. praematurus* has been entirely replaced by *Par. acuminatus.* The varied, not always favourable mode of preservation and co-occurrence of the two parakidograptid morphotypes is the reason that we prefer a combined *ascensus–acuminatus* Biozone instead of separate, but imperfectly distinguished *ascensus* and *acuminatus* biozones.

The appearance of typical 'Gondwanan' faunal assemblages relatively high in the Estana black shale succession and the absence of the earlier O–S boundary assemblages with *N. lubricus*, *N. rhizinus*, *N.* aff. *rhizinus*, *N. minor*, *N. baridaensis*, *N. ednae*, *K. bifurcus*, *K. bicaudatus*, *K. lanpherei* and *Nd. shanchongensis* in other stratigraphically relevant black shale sections of northern peri-Gondwana may be alternatively explained by either immigration of exotic graptolite taxa under specific local environmental conditions or widespread omission of corresponding graptolitic black shale strata in many peri-Gondwanan sections. The absence of these taxa is in notable conjunction with condensed, discontinuous or oxic sedimentation, whereas their presence, although usually incomplete, is linked with less condensed and presumably continuous black shale sedimentation that commenced well before the appearance of the first akidograptids.

The faunal affinity of a single interval with well-determinable graptolite taxa in the Austrian Southern Alps to the lower part of the *ascensus–acuminatus* Biozone in the Estana section matches this assumption, although poor graptolite preservation in other levels of the Austrian section precludes full evidence. Determinable graptolites found in siliceous black shale *c.* 1 m above the top of the underlying quartzite bed in Austria included *K. bifurcus*, *Par. praematurus* and simple normalograptids, whereas *Nd. lanceolatus*, *N. trifilis*, *Cyst. ancestralis* and other elements of Assemblage 4 are missing. Black shales and lydites below this fossiliferous level may be correlative with the upper *persculptus* (*parvulus*) Biozone of the Estana section; black shales above the fossiliferous level could be assigned to the middle part of the *ascensus–acuminatus* Biozone, although direct faunal evidence is not preserved. Condensed sedimentation, disconformities and an incomplete fossil record observed in many other sections can be explained by sediment starvation associated with a rapid and culminating post-glacial rise in sea-level (see Melchin *et al.* 2013 for review). In the Prague Synform of central Bohemia, for instance, condensed sedimentation or non-deposition at the interface between upper-Hirnantian mudstones and lowest Silurian black shales has been presumed by Štorch (2006), prior to the indirect evidence provided by the Estana section. In

central Bohemia the uppermost Hirnantian oxic mudstones with *Hirnantia* fauna and *M. persculptus*, Assemblage 1 in Figure 5, are topped by a firmground (Štorch, 2006) overlain by black shale with abundant *Nd. lanceolatus*, *A. ascensus*, *N. angustus*, *G. dufkai* (Assemblage 3a), 0.1–0.2 m higher joined by *N. trifilis*, *Cyst. ancestralis*, *Neodiplograptus parajanus* (Štorch, 1983) and *Par. acuminatus* (Assemblage 4). A black shale succession from the *parvulus* and lowermost *ascensus–acuminatus* biozones correlative with those of the Spanish Estana and Austrian Waterfall sections is missing in the Prague Synform.

The record of a single specimen of *Hirsutograptus*, a genus previously unknown from Europe (other than Scotland), within a graptolite assemblage characteristic of the lower-middle *ascensus–acuminatus* Biozone in northern Gondwana, suggests that this level may be tentatively correlatable with the *Hirsutograptus sinitzini* Subzone recognized high in the *ascensus–acuminatus* Biozone of Asia and northern North America and with the lower part of the *acuminatus* Biozone of Yukon Territory, Canada (*sensu* Loxton, 2017). Poorly preserved *Hirsutograptus* sp. from the Estana section is similar to relatively small multispinous hirsutograptids including *Hirsutograptus comantis* (Chaletskaya, 1960), *Hirsutograptus sinitzini* (Chaletskaya, 1960) and *Hirsutograptus villosus* Koren' & Rickards, 1996.

7. Conclusions

The Ordovician–Silurian boundary section near Estana village in the south-central Pyrenees of Spain exposes richly fossiliferous black shales little affected by faulting or tectonic strain and sheds new light on high-resolution biostratigraphy and global correlation of the boundary interval world-wide. Increasing and little fluctuating TOC content (1.8–3.2 wt. %), $\delta^{13}C_{org}$ values decreasing with some fluctuation from -29.84 ‰ to -30.60 ‰, and gradual replacement of graptolite assemblages is in conformity with presumably uninterrupted anoxic sedimentation within a single graptolite biofacies.

We have recognized and defined a distinct *Metabolograptus parvulus* Biozone correlatable with the uppermost part of *Metabolograptus persculptus* Biozone including also the so-called pre-*ascensus* interval with *Normalograptus avitus* Fauna recognized by Koren', Ahlberg & Nielsen (2003) below the FADs of *A. ascensus* and *Par. praematurus*.

A combined *Akidograptus ascensus–Parakidograptus acuminatus* Biozone has been adopted in the lowermost part of the Silurian succession instead of separate *ascensus* and *acuminatus* biozones because the two index taxa overlap for a large part of their stratigraphical ranges. In addition, *Par. praematurus*, which is difficult to distinguish when unfavourably preserved from early specimens assigned to *Par. acuminatus*, has its lowest occurrence in the same sample as *A. ascensus*.

High-diversity graptolite faunas of the *parvulus* and lower–middle *ascensus–acuminatus* biozones comprise 27 species including two new taxa (*Normalograptus baridaensis* sp. nov. and *Normalograptus ednae* sp. nov.) and several taxa of particular biostratigraphical

significance in Siberia, central Asia, China and northern North America, i.e. in lower-latitudes of the early Llandovery Earth palaeogeographical reconstruction by Torsvik & Cocks (2017, fig. 7.1a).

A succession of four graptolite assemblages is recognized in the O–S boundary interval comprising *persculptus* (herein *parvulus*) and lower – middle *ascensus-acuminatus* biozones (Fig. 5). The lowest one marked by the occurrence of *M. persculptus* (Assemblage 1) is missing in the black-shale Estana section. Only the fourth assemblage, recorded in the uppermost part of the studied succession, is fully represented in all relevant sections in peri-Gondwanan Europe. The high number of graptolite taxa recorded in the Estana section for the first time in peri-Gondwanan Europe (in particular *N. minor*, *N. lubricus*, *N. mirnyensis*, *N. rhizinus*, *N.* aff. *rhizinus*, *M. parvulus*, *Hirsutograptus* sp., *K. bicaudatus*, *K. bifurcus*, *K. lanpherei*, *Nd. shanchongensis* and *Par. praematurus*) and the presence of two new species (*N. ednae, N. baridaensis*), might be explained by the local occurrence of specific environmental conditions which, along with indigenous speciation, allowed for the immigration of several truly exotic taxa. Although the black-shale facies is closely similar to those elsewhere in peri-Gondwanan Europe, somewhat specific conditions in the latest Hirnantian may be inferred from the presence of abnormal split and uniserial rhabdosomes and the common occurrence of synrhabdosomes.

However, many of the 'exotic' graptolite taxa previously known only from low-latitude palaeoplates are actually cosmopolitan and their general absence in other sections of peri-Gondwanan Europe leads us to assume that the lower 2–3 m of the black shale succession studied in the Estana section, with their highly distinctive graptolite assemblages of the *parvulus* and lowermost *ascensus–acuminatus* biozones (Assemblage 2 and fully developed Assemblage 3), represent strata which are either oxic and barren of graptolites, condensed or even missing elsewhere in peri-Gondwanan Europe.

8. Palaeontological notes

Normalograptus lubricus (Chen & Lin, 1978)

Specimens assigned to *N. lubricus* (Figs. 3a–c) are confined in a narrow stratigraphical interval below the lowest occurrence of akidograptids in the Estana section. Proximal end of the rhabdosome is furnished with rather short virgella and one or two basal spines growing from the upward turning point of the th1^1. Maximum width of 0.95-1.05 mm, attained with 5th thecal pair is lesser than that measured by Koren' & Melchin (2000) in specimens from Uzbekistan but still greater than maximum width of *N. lubricus* from Dob's Linn [see *Climacograptus* sp. (aff. *C. miserabilis*) of Williams (1983)]. Number of basal spines documented by other authors (2–4 including virgella) depends on burial and flattening of the rhabdosome since many specimens are preserved in subscalariform view and spines were projected in various directions, not simply parallel to the rhabdosome profile view.

***Normalograptus minor* (Huang, 1982)**

Abundant specimens of *N. minor* (Figs. 3r–u; 10e, p) attain a maximum length of 34 mm, excluding the long and robust, 0.1–0.18 mm wide, nema, and 3–5 mm long virgella which splits into multiple, up to 1.3 mm long, densely packed root-like branches. The proximal end is sub-rounded, slightly asymmetrical, 0.9–1.15 mm wide at the level of th1¹–th1² apertures. The rhabdosome gradually widens until the maximum width of *c*. 1.5–1.6 mm is attained by the 9th–10th thecal pair. Extreme values range from 1.3 mm to 1.95 mm depending on rhabdosome orientation relative to the tectonic strain. Thecae are strongly geniculated; narrow thecal excavations occupy about one-third of the rhabdosome width. Supragenicular walls are slightly inclined in most specimens. Two thecae repeat distance (2TRD) is 1.5–1.75 mm at th2 and 1.8–2.0 mm at th10. Distal thecae number 10–11 in 10 mm. Relatively short specimens in the same bedding plane assemblages exhibit lesser maximum width (1.1 mm), slightly more densely packed thecae (12 in 10 mm), and shorter virgellae, although terminated by an identical root-like furcation. The type specimens of *N. minor* from Tibet are rather small, with 6 thecae in 5 mm of rhabdosome length and a maximum width of 1.2–1.3 mm (Huang, 1982). Their virgella forked 3.5–5.5 mm below the sicular aperture into several isolated branches. All specimens are characterized by a long, forked virgella, long nema and slight and gradual widening of the rhabdosome. Also the scalariform specimen of *Normalograptus* sp. B, recorded by Štorch & Serpagli (1993, text-fig. 7P) from the *ascensus–acuminatus* Biozone of south-western Sardinia, may be tentatively assigned to *N. minor*. *Climacograptus radicatus* Chen & Lin, 1978 and *Diplograptus coremus* Chen & Lin, 1978, other species with long multifurcated virgella which occur in Ordovician–Silurian boundary beds, can be readily distinguished from *N. minor* by their robust rhabdosomes, widening from 0.6–0.7 mm at th1 to a distal maximum of 2.2–2.4 mm, bluntly geniculated thecae with markedly inclined supragenicular walls, wider thecal spacing, with a 2TRD of 2.3–2.4 mm, and virgella branched into few, relatively long branches (see also Chen & Lin, 1978). Chen *et al*. (2005) regarded *Cl. radicatus* as a junior synonym of *Neodiplograptus coremus* (Chen & Lin, 1978).

***Normalograptus* aff. *rhizinus* (Li & Yang in Nanjing Institute of Geology and Mineral Resources, 1983)**

Normalograptus aff. *rhizinus* (Figs. 3o, p; 10r) matches *N. rhizinus* in having a rhabdosome widening gradually from 0.75–0.8 mm at the first thecal pair to a maximum of 1.55–1.7 mm which is attained by the 10th–14th thecal pair. The long virgella widens distally into a vane-like structure. However, the virgella of *N.* aff. *rhizinus* is slender and the vane structure, when preserved, is confined to its distal part. Distal thecae are long and widely spaced in *N.* aff. *rhizinus* with a 2TRD at th10 of 2.6–3.0 mm as opposed to the 1.8–2.5 mm recorded in *N. rhizinus*.

Metabolograptus parvulus (Lapworth, 1900)

Abundant material assigned to *M. parvulus* (Figs. 3d, g–i; 10c–d) differs from the closely similar *Metabolograptus persculptus* as shown by Štorch & Loydell (1996), Loydell *et al.* (2002), Loydell (2007) and Blackett *et al.* (2009) in possessing a narrower rhabdosome, less overlapping thecae and closer thecal spacing. The maximum width of the present flattened rhabdosomes, including those oriented parallel or perpendicular to the tectonic strain, varies between 1.5 mm and 1.75 mm, 2TRD at th2 is 1.2–1.35 mm and 2TRD at th10 is 1.3–1.55 mm.

Korenograptus bifurcus (Mu *et al.*, 1974)

The abundant large rhabdosomes of *K. bifurcus* (Figs. 7c, k; 8g, ?j; 10a) possess a long and robust virgella bifurcating 3.0–6.5 mm below the sicular aperture into two equally robust, 10–15 mm long branches. The absence of rhabdosomes preserved in scalariform or sub-scalariform view suggests that the plane of bifurcation was parallel to the rhabdosome profile view. Thecae are gently geniculated, acuminate in profile view, having a convex supragenicular wall and aperture perpendicular to the rhabdosome axis. The proximal end is bluntly triangular, 1.0–1.15 mm wide at the level of th1^1–th1^2 apertures. A maximum width of 2.4–2.65 mm is attained by the 10th–15th thecal pair. In several specimens a robust nema splits into a large irregular net-like, probably membranous structure. Similar irregular branching developed on the forked virgella of the specimen questionably assigned to this species illustrated in Fig. 8j. Material from the Austrian Southern Alps was identified as *Rickardsograptus*? *bifurcus* (Ye, 1978) by Štorch & Schönlaub (2012), but further examination of the Chinese material suggests that ‘*Glyptograptus bifurcus*’ Ye, 1978 as well as ‘*Orthograptus*’ *lonchoformis* Chen & Lin, 1978 and ‘*Orthograptus furcatus*’ Ye in Jin *et al.*, 1982 are conspecific with the senior synonym ‘*Diplograptus bifurcus*’ Mu *et al.*, 1974. The pattern H early astogeny, largely glyptograptid thecae with little change of geniculation throughout the relatively slowly widening rhabdosome, lack of genicular thickening and rather late origin of the median septum refer this, and related species to the genus *Korenograptus* defined by Melchin *et al.* (2011).

Korenograptus bicaudatus (Chen & Lin, 1978)

Specimens assigned to this species (Figs. 8a, r, ?i; 10s) match the type material of ‘*Climacograptus*’ *bicaudatus* figured by Chen & Lin (1978, pl. 5, figs 10, 11) and refigured by Mu *et al.* (2002, pl. 176, figs 3, 4). *Korenograptus bicaudatus* is characterized by its short virgella forked 0.25–0.5 mm from the sicular aperture into two long, ventrally directed and only slightly curved branches. The rhabdosome widens gradually from 0.9–1.1 mm at th1 to a maximum of 2.1–2.3 mm in profile view attained by th16–20. Scalariform specimens barely attain 2.0 mm in width. The 2TRD increases from 2.0 mm at th2 to 2.2–2.5 mm in distal thecae of mature, more than 30 mm long specimens. The short virgella and relatively narrow and deeply incised apertural excavations enable *K. bicaudatus* to be distinguished from other

taxa with a bifurcated virgella described from the same level (*ascensus–acuminatus* Biozone) in China. The species, formerly assigned to *Climacograptus*, is commonly preserved in subscalariform view but a specimen preserved in profile view (Fig. 8r) reveals its thecal geniculation and inclined supragenicular walls resembling other similar species herein assigned to *Korenograptus*.

Korenograptus lanpherei (Churkin & Carter, 1970)

Robust rhabdosomes (Figs. 7h; 8f, l; 10m) attaining a length of *c.* 60 mm in full maturity match material described by Loxton (2017) in most characters and measurable parameters including width and 2TRD. Greater maximum width, up to 2.9 mm, occurs in mature specimens flattened in full profile. The sub-triangular proximal end is furnished with a robust, more than 12 mm long virgella without any bifurcation. The ascending part of its th1^1 is inclined at an angle of 17–19° to the rhabdosome axis. Subsequent thecae possess rounded, glyptograptid genicula and straight or slightly convex supragenicular walls inclined at 23–38°. Low values occur in slightly subcalariform specimens and/or specimens oriented more nearly parallel to the principal elongation. Thecal apertures are horizontal and each occupies one-quarter of the rhabdosome width. Two thecae repeat distance attains 2.2–2.55 mm in the distal part of particularly long rhabdosomes. *Korenograptus lanpherei* differs from its stratigraphic predecessor *K. bifurcus* in having a very long but simple virgella. *Korenograptus bicaudatus* possesses a short bifurcated virgella, lesser rhabdosome width and more geniculated thecae. The plane of virgellar bifurcation is probably oblique or perpendicular to the rhabdosome profile. The long and robust virgella, longer ascending part of th1^1, less geniculated thecae and greater width of its rapidly widening rhabdosome differentiate *K. lanpherei* from the otherwise similar *Korenograptus lungmaensis* (Sun, 1933) although a rhabdosome from the base of the *ascensus* Biozone, assigned to the latter species by Chen, Rong & Fan (2003, fig. 1H), also possesses a long virgella, triangular proximal end and robust nema. This form also resembles *Nd. parajanus* in general rhabdosome appearance and many measurable parameters (rhabdosome width, early astogeny of pattern H, thecal spacing, long robust undivided virgella and nema) but can be readily distinguished by its sub-triangular proximal end and uniform glyptograptid thecae with flowing genicula throughout the rhabdosome. The thecae of *Nd. parajanus*, by comparison, are markedly biform: strongly geniculated, almost climacograptid in the proximal part of the rhabdosome and nearly orthograptid distally.

Neodiplograptus shanchongensis (Li, 1984)

Neodiplograptus shanchongensis from the *persculptus* and lower *ascensus–acuminatus* biozones of China (Li, 1984; Chen *et al.* 2000, 2005), Arctic Canada (Melchin, McCracken & Oliff, 1991), southern Scotland (Fan, Melchin & Williams, 2005), Jordan (Loydell, 2007) and Saudi Arabia (Williams *et al.* 2016) can be differentiated from the rather similar *Nd. lanceolatus* by its thecal geniculation developed until the distal part of the rhabdosome, less steeply inclined supragenicular walls and more parallel-sided rhabdosome widening from 1.3–1.4 mm at the first thecal pair to a maximum of 2.1 mm attained by th8–10. New records from

the Estana section (Figs. 7p, x; 10g, o) suggest that *Nd. shanchongensis* may be the stratigraphical praecursor of *Nd. lanceolatus* which appears in abundance higher, still in the lower, but apparently not the lowermost part of the *ascensus–acuminatus* Biozone.

Parakidograptus praematurus (Davies, 1929)

Specimens of *Par. praematurus* (Figs. 7e, i; 8b, p; 10n), which are fairly common in the lower part of the *ascensus-acuminatus* Biozone, are distinguished from early populations of *Par. acuminatus* (Figs 7d, aa; 10k) by their less exposed sicula, lower position of thl[1] bud on the sicula (< 0.2 mm from the sicular aperture), usually lesser maximum width (1.5 mm), and generally less protracted proximal end. Thecae are more geniculated throughout the rhabdosome when compared with flattened *Par. acuminatus*. *Parakidograptus praematurus* also lacks the acuminate thecal apertural margins typical of *Par. acuminatus* including its stratigraphically lowest specimens which are marked by a less protracted proximal part and lesser rhabdosome width (< 2.0 mm) than the stratigraphically higher specimens recorded from this locality above the measured section. *Akidograptus ascensus* can be distinguished from our specimens assigned to *Par. praematurus* by its less inclined supragenicular thecal walls, usually lesser maximum width (0.8–1.2 mm), and more protracted proximal end with long exposed sicula and turning point of th1[1] situated *c*. 0.5 mm above the sicular aperture.

9. Systematic part

Normalograptus baridaensis sp. nov. (page 1087)
Figs. 3j–k, m; 10 ?l, q

Derivation of name. After el Baridà, the small region of the upper Segre valley in which the Estana section is located and where the Late Ordovician stratigraphical units of the central Pyrenees were defined.

Holotype. MGM-8096-O (Figs. 3j, 10q) from Sample EST 2b, in the uppermost Hirnantian *M. parvulus* Biozone of the Estana section, central Pyrenees, Lleida Province, Spain.

Material. Twelve flattened specimens with proximal end furnished with virgella and secondary basal spine.

Diagnosis. Slender, 0.9 – 1.1 mm wide *Normalograptus* with long virgella and single straight secondary spine projecting with low angle of divergence from base of 0.4–0.6 mm long robust part of virgella.

Description. The slender, only 0.9–1.1 mm wide, parallel-sided rhabdosome of *N. baridaensis* is furnished with a 4–6 mm long virgella with a considerably thickened 0.4–0.6 mm long basal part and a single, straight, 2–4 mm long secondary spine projecting from the end of the thickened part of the virgella with an angle of divergence ranging usually from 4° to 5°.

18

Alternating normalograptid thecae are strongly geniculated with gently inclined supragenicular walls, asymmetrical apertural excavations and a 2TRD ranging from 2.1 mm to 2.6 mm at the level of th10.

Remark. This uncommon form from the uppermost part of the *parvulus* (i.e. upper *persculptus*) Biozone can be distinguished from *N. bifurcatus* Loydell, 2007 by its wider thecal spacing and lack of any bifurcated antivirgellar spine.

Normalograptus ednae **sp. nov.** (page 1087)
Figs. 7g, q, bb; 8q; 10b, f

Derivation of name. After the feminine name Edna, the second author's granddaughter.

Holotype. MGM-1761-S (Figs. 7q, 10b) from Sample EST 16, lowermost Rhuddanian lower *ascensus-acuminatus* Biozone of the Estana section, central Pyrenees, Lleida Province, Spain.

Material. Twelve mature specimens with proximal end, virgella and lateral spines and several incomplete or immature rhabdosomes.

Diagnosis. *Normalograptus* gradually widening from 0.7 mm at first thecal pair to distal maximum of 1.5 mm, with strongly geniculated thecae, parallel-sided supragenicular thecal walls, short and robust virgella and two claw-like lateral spines originating from the upward turning point of th1^1.

Description. Rhabdosome attaining length of *c.* 20–25 mm widens gradually from 0.7 mm at the level of the first thecal pair apertures, through 0.95–1.05 mm at th5, and 1.2–1.3 mm at th10 to a maximum of 1.5 mm attained by the 13th –17th theca. The slightly asymmetrical proximal end is furnished with a 0.2–1.5 mm long virgella and two equally short and robust, somewhat claw-like curved lateral spines. Spines grew from the upward turning point of th1^1, probably parallel to the ventral margins of the rhabdosome. The upward growing part of th1^2 is relatively long (1.0–1.2 mm) compared to the narrow proximal end of the rhabdosome. Alternating climacograptid thecae exhibit parallel-sided supragenicular walls, sharp genicula and slightly asymmetrical apertural excavations. Two thecae repeat distance ranges from 1.8 mm to 2.5 mm throughout the rhabdosome, depending on the tectonic strain.

Discussion. *Normalograptus ednae* can be distinguished from *N. trifilis* by its narrower rhabdosome, gradually widening to a lesser maximum width of 1.5 mm compared to 2.0 mm in the latter species. The basal spines of *N. ednae* are short, robust and slightly curved whereas both the virgella and basal spines of *N. trifilis* are long, slender and almost straight. In the Estana section, *N. ednae* is confined to a narrow stratigraphical interval in the lower part of the *ascensus–acuminatus* Biozone, below the FAD of *N. trifilis* which is a typical faunal component of the lower–middle *ascensus–acuminatus* Biozone.

References

BERGSTRÖM, S. M., HUFF, W. D., KOREN', T. N., LARSSON, K., AHLBERG, P. & KOLATA, D. R. 1999. The 1997 core drilling through Ordovician and Silurian strata in Röstanga, S. Sweden: Preliminary stratigraphic assessment and regional comparison. *GFF* **121**, 127–35.

BJERRESKOV, M. 1975. Llandoverian and Wenlockian graptolites from Bornholm. *Fossils and Strata* **8**, 1–94.

BLACKETT, E., PAGE, A., ZALASIEWICZ, J., WILLIAMS, M., RICKARDS, B. & DAVIES, J. 2009. A refined graptolite biostratigraphy for the late Ordovician – early Silurian of central Wales. *Lethaia* **42**, 83–96.

BOISSEVAIN, H. 1934. Étude géologique et géomorphologique d'une partie de la vallée de la Haute Sègre (Pyrénées Catalanes). *Bulletin de la Société d'Histoire Naturelle de Toulouse* **66**, 33–170.

CASAS, J. M. 2010. Ordovician deformations in the Pyrenees: new insights into the significance of pre-Variscan ('sardic') tectonics. *Geological Magazine* **147**, 674–89.

CASAS, J. M. & PALACIOS, T. 2012. First biostratigraphical constraints on the pre-Upper Ordovician sequences of the Pyrenees based on organic-walled microfossils. *Comptes Rendus Geoscience* **344**, 50–6.

CASAS, J.M., PUDDU, C. & ÁLVARO, J. J. 2017. Fieldtrip to eastern Pyrenees, Catalonia and Occitanie, Stop 7a. Upper Ordovician succession in Talltendre. *Géologie de la France* **2017** (1), 43–6.

CHALETSKAYA, O. N. 1960. New species of the Llandovery graptolites of Central Asia. In *Novye Vidy Drevnikh Rastenii i Bespozvonochnykh SSSR, Chast 2*. (ed. B. P. Markovsky), pp. 373–5. Gosudarstvennoe Naucho-teknicheskoje Izdatelstvo, Moskva. [in Russian]

CHEN, X. 1984. Silurian graptolites from Southern Shaanxi and northern Sichuan with special reference to classification of Monograptidae. *Palaeontologia Sinica 166*, *New Series B* **20**, 1–102.

CHEN, X. & LIN, Y. K. 1978. Lower Silurian graptolites from Tongzi, northern Guizhou. *Memoir of the Nanjing Institute of Geology and Palaeontology, Academia Sinica* **12**, 1–106. [in Chinese with English Abstract]

CHEN, X., RONG, J. Y. & FAN, J. X. 2003. A proposal for a candidate section for restudy of the base of Silurian. In *Proceedings of the 7th International Graptolite Conference and Field Meeting of the ISSS* (eds G. Ortega & G. F. Aceñolaza), pp. 119–23. *INSUGEO, Serie Correlación Geológica* **18**.

CHEN, X., FAN, J. X., MELCHIN, M. J. & MITCHELL, C. E. 2005. Hirnantian (latest Ordovician) graptolites from the Upper Yangtze Region, China. *Palaeontology* **48**, 235–80.

CHEN, X., RONG, J. Y., MITCHELL, C. E., HARPER, D. A. T., FAN, J. X., ZHAN, R. B., ZHANG, Y. D., LI, R. Y. & WANG, Y. 2000. Late Ordovician to earliest Silurian graptolite and brachiopod biozonation from the Yangtze region, South China, with a global correlation. *Geological Magazine* **137**, 623–50.

CHURKIN JR, M. & CARTER, C. 1970. Early Silurian graptolites from southeastern Alaska and their correlation with graptolitic sequences in North America and the Arctic. *United States Geological Survey Professional Paper* **653**, 1–51.

COLMENAR, J. 2015. The arrival of brachiopods of the *Nicolella* Community to the Mediterranean margin of Gondwana during the Late Ordovician: Palaeogeographical and palaeoecological implications. *Palaeogeography, Palaeoclimatology, Palaeoecology* **428**, 12–20.

DALLONI, M. 1930. Étude géologique des Pyrénées catalanes. *Annales de la Faculté des Sciences de Marseille* **26**, 1–373.

DAVIES, K. A. 1929. Notes on the graptolite faunas of the Upper Ordovician and Lower Silurian. *Geological Magazine* **66**, 1–27.

DÉGARDIN, J.-M. 1988. Le Silurien des Pyrénées. Biostratigraphie. Paléogéographie. *Société Géologique du Nord*, Publication **15**, 506 pp.

DÉGARDIN, J.-M. 1990. The Silurian of the Pyrenees. *Journal of the Geological Society* **147**, 687–92.

DÉGARDIN, J.M. (coord.), ALONSO, J.L., BESSIÈRE, G., BODIN, J., BOUQUET, G., BRULA, P., CENTÈNE, A., DURAN, H., GARCES-COCCHIO, A.M., GARCÍA-LÓPEZ, S., GARCÍA-SANSEGUNDO, J., GUÉRANGÉ, B., JULIVERT, M., LAUMONIER, B., LOSANTOS, M., PALAU, J., PARIS, F., POUIT, G., RAYMOND, D., RICHARD, P., SANZ, J., TRUYOLS-MASSONI, M. & VILLAS, E. 1996. Ordovicien Supérieur – Silurien. In *Synthèse géologique et géophysique des Pyrénées*. (eds A. Barnolas & J. C. Chiron), pp. 211–33. Bureau de Recherches Géologiques et Minières – Instituto Geológico y Minero de España.

DELABROYE, A., MUNNECKE, A., SERVAIS, T., VANDENBROUCKE, T. R. A. & VECOLI, M. 2012. Abnormal forms of acritarchs (phytoplankton) in the upper Hirnantian (Upper Ordovician) of Anticosti Island, Canada. *Review of Palaeobotany and Palynology* **173**, 46–56.

ELLES, G. L. & WOOD, E. M. R. 1907. A monograph of British graptolites. Part 6. *Monograph of the Palaeontographical Society* **61** (297), 217–72.

FAN J. X., PENG, P. & MELCHIN, M. J. 2009. Carbon isotopes and event stratigraphy near the Ordovician–Silurian boundary, Yichang, South China. *Palaeogeography, Palaeoclimatology, Palaeoecology* **276**, 160–9.

FAN, J. X., MELCHIN, M. J. & WILLIAMS, S. H. 2005. Restudy of the Hirnantian (latest Ordovician) graptolites from Dob's Linn, southern Scotland. In *Abstracts for the Second International Symposium of IGCP 503 on Ordovician Palaeogeography and Palaeoclimate* (eds P. T. Sheehan & T. Servais), pp. 7–8. *Milwaukee Public Museum Series in Natural History* 2.

GIL-PEÑA, I. & BARNOLAS, A. 2007. A review of the Ordovician sequence in the Pyrenean Axial Zone and the Catalonian Coastal Ranges, NE Iberia. In *IGCP Project 503. Regional Meeting and Field-trip*, pp. 11–2. Publicaciones Universidad de Zaragoza.

GIL-PEÑA, I., BARNOLAS, A., SANZ-LÓPEZ, J., GARCÍA-SANSEGUNDO, J. & PALAU, J. 2001. Discontinuidad sedimentaria del Ordovícico terminal en los Pirineos centrales. *Geogaceta* **29**, 57–60.

GIL-PEÑA, I., BARNOLAS, A., VILLAS, E. & SANZ-LÓPEZ, J. 2004. El Ordovícico Superior de la Zona Axial. In *Geología de España* (ed. J.A. Vera), pp. 247–9. SGE-IGME, Madrid.

GOGIN, I. J., KOREN', T. N., PEGEL', T. V. & SOBOLEVSKAYA, R. F. 1997. *Atlas zonalnykh kompleksov veduschikh grup rannepaleozoiskoy fauny severa Rossii*. Izdatelstvo VSEGEI, Sankt-Petersburg. 205 pp. [in Russian]

GUTIÉRREZ-MARCO, J. C. & LENZ, A. C. 1998. Graptolite synrhabdosomes: biological or taphonomic entities? *Paleobiology* **24**, 37–48.

GUTIÉRREZ-MARCO, J. C. & ROBARDET, M. 1991. Découverte de la Zone à *Parakidograptus acuminatus* (base du Llandovery) dans le Silurien du Synclinorium de Truchas (Zone asturo-léonaise, Nord-Ouest de l'Espagne): consequences stratigraphiques et paléogéographiques au passage Ordovicien–Silurien. *Comptes Rendus de l'Academie des Sciences, Paris, Série H* **312**, 729–734.

HARTEVELT, J. J. A. 1970. Geology of the Upper Segre and Valira valleys, central Pyrenees, Andorra/Spain. *Leidse Geologische Mededelingen* **45**, 167–236.

HUANG, Z. G. 1982. Latest Ordovician and earliest Silurian graptolite assemblages of Xainza district, Xizang (Tibet) and Ordovician-Silurian boundary. In *Contribution to the geology of the Qinghai-Xizang (Tibet) plateau*, 7. (ed. Editorial Committee of Ministry of Geology and Mineral Resources), pp. 27–52. Geological Publishing House, Beijing. [in Chinese, English abstract]

HUTT, J. E. 1974. The Llandovery graptolites of the English Lake District. Part 1. *Monograph of the Palaeontographical Society* **128** (540), 1–56.

INSTITUT GEOLÒGIC DE CATALUNYA AND INSTITUT CARTOGRÀFIC DE CATALUNYA (ed.) 2010. Atles Geològic de Catalunya. 463 pp.

JAEGER, H. 1977. Das Silur/Lochkov-Profil im Frankenberger Zwischengebirge (Sachsen). *Freiberger Forschungshefte*, C **326**, 45–59.

JAEGER, H., HAVLÍČEK, V. & SCHÖNLAUB, H.-P. 1975. Biostratigraphie der Ordovizium/Silur Grenze in den Südalpen – Ein Beitrag zur Diskussion um die Hirnantia-Fauna. *Verhandlungen der Geologischen Bundesanstalt* **1975**, 271–89.

JAEGER, H. & ROBARDET, M. 1979. Le Silurien et le Devonien basal dans le nord de la province de Séville (Espagne). *Geobios* **12**, 687–714.

JIN, C. T., YE, S. H., HE, Y. X., WAN, Z. Q., WANG, S. B., ZHAO, Y. T., LI, S. J., XU, X. Q. & ZHANG, Z. Q. 1982. *The Silurian stratigraphy and palaeontology in Guanyinqiao, Qijiang, Sichuan.* People`s Publishing House of Sichuan, Chengdu. 84 pp. [in Chinese with English abstract]

KOREN', T. N. & BJERRESKOV, M. 1997. Early Llandovery monograptids from Bornholm and the southern Urals: taxonomy and evolution. *Bulletin of the Geological Society of Denmark* **44**, 1–43.

KOREN', T. N. & MELCHIN, M. J. 2000. Lowermost Silurian graptolites from the Kurama Range, eastern Uzbekistan. *Journal of Paleontology* **74**, 1093–113.

KOREN', T. N. & RICKARDS, R. B. 1996. Taxonomy and evolution of Llandovery biserial graptoloids from the southern Urals, western Kazakhstan. *Special Papers in Palaeontology* **54**, 1–103.

KOREN', T. N., AHLBERG, P. & NIELSEN, A. T. 2003. The post-*persculptus* and pre-*ascensus* graptolite fauna in Scania, south-western Sweden: Ordovician or Silurian? In *Proceedings of the 7th International Graptolite Conference and Field Meeting of the ISSS* (eds G. Ortega & G. F. Aceñolaza), pp. 133–8. *INSUGEO, Serie Correlación Geológica* **18**.

KRSTIČ, B., MASLAREVIČ, L. & SUDAR, M. 2005. On the Graptolite Schists Formation (Silurian – Lower Devonian) in the Carpatho-Balkanides of eastern Serbia. *Annales Géologiques de la Péninsule Balkanique* **66**, 1–8.

LAKOVA, I. & SACHANSKI, V. 2004. Cryptospores and trilite spores in oceanic graptolite-bearing sediments (Saltar Formation) across the Ordovician–Silurian boundary in the West Balkan Mountains, Bulgaria. *Review of the Bulgarian Geological Society* **65**, 151–6.

LAPWORTH, H. 1900. The Silurian sequence of Rhayader. *Quarterly Journal of the Geological Society of London* **56**, 67–137.

LEGRAND, P. 1977. Contribution à l'etude des graptolites du Llandoverien inferieur de l'Oued In Djerane (Tassili N'ajjer oriental, Sahara algérien). *Bulletin de la Société d'Histoire Naturelle de l'Afrique du Nord* **67**, 141–96.

LI, J. J. 1984. Graptolites across the Ordovician–Silurian boundary from Jingxian, Anhui. In *Stratigraphy and palaeontology of systemic boundaries in China. Ordovician-Silurian boundary (1)* (ed. Nanjing Institute of Geology and Palaeontology), pp. 309–70. Anhui Science and Technology Publishing House, Hefei.

LOXTON, J. D. 2017. Graptolite diversity and community changes surrounding the Late Ordovician mass extinction: high resolution data from the Blackstone River, Yukon. PhD thesis, Dalhousie University, Halifax, Canada. Published thesis.

LOYDELL, D. K. 2007. Graptolites from the Upper Ordovician and lower Silurian of Jordan. *Special Papers in Palaeontology* **78**, 1–66.

LOYDELL, D. K., MALLETT, A., MIKULIC, D. G., KLUESSENDORF, J. & NORBY, R. D. 2002. Graptolites from near the Ordovician–Silurian boundary in Illinois and Iowa. *Journal of Paleontology* **76**, 134–37.

MANCK, F. 1923. Untersilurische Graptolithenarten der Zone 10, ferner *Diversograptus* gen. nov., sowie einige neue Arten anderer Gattungen. *Die Natur* **14**, 282–89.

MARGALEF, A., CASTIÑEIRAS, P., CASAS, J. M., NAVIDAD, M., LIESA, M., LINNEMANN, U., HOFMANN, M. & GÄRTNER, A. 2016. Detrital zircons from the Ordovician rocks of the Pyrenees: Geochronological constraints and provenance. *Tectonophysics* **681**, 124–34.

MASIAK, M., PODHAŁAŃSKA, T. & STEMPIEŃ-SAŁEK, M. 2003. Ordovician – Silurian boundary in the Bardo Syncline (Holy Cross Mountains) – new data on fossil assemblages and sedimentary succession. *Geological Quarterly* **47**, 311–29.

MELCHIN, M. J. 1989. Llandovery graptolite biostratigraphy and paleobiogeography, Cape Phillips Formation, Canadian Arctic Islands. *Canadian Journal of Earth Sciences* **26**, 1726–46.

MELCHIN, M. J. 2001. The GSSP for the base of the Silurian System. *Silurian Times* **9**, 36-41.

MELCHIN, M.J. 2003. Restudying a global stratotype for the base of the Silurian: a progress report. In *Proceedings of the 7th International Graptolite Conference and Field Meeting of the ISSS* (eds G. Ortega & G. F. Aceñolaza), pp. 147–9. *INSUGEO, Serie Correlación Geológica* **18**.

MELCHIN, M. J., MCCRACKEN, A. D. & OLIFF, F. J. 1991. The Ordovician–Silurian boundary on Cornwallis and Truro islands, Arctic Canada: preliminary data. *Canadian Journal of Earth Sciences* **28**, 1854–62.

MELCHIN, M. J., MITCHELL, C. E., HOLMDEN, C. & ŠTORCH, P. 2013. Environmental changes in the Late Ordovician–early Silurian: Review and new insights from black shales and nitrogen isotopes. *The Geological Society of America Bulletin* **125**, 1635–70.

MELCHIN, M. J., MITCHELL, C. E., NACZK-CAMERON, A., FAN, J. X. & LOXTON, J. 2011. Phylogeny and adaptive radiation of the Neograptina (Graptoloida) during the Hirnantian mass extinction and Silurian recovery. *Proceedings of the Yorkshire Geological Society* **58**, 281–309.

MU, E. Z., LI, J. J., GE, M. Y., LIN, Y. K. & NI, Y. N. 2002. *Graptolites of China*. Science Press, Beijing, 1205 pp. [in Chinese]

MUIR, L. A. 2011. An unusual specimen of *Glyptograptus* from Dob's Linn (Southern Uplands, Scotland), and a discussion of graptolites teratomorphies. *Proceedings of the Yorkshire Geological Society* **58**, 311-7.

MUNNECKE, A., DELABROYE, A., SERVAIS, T., VANDENBROUCKE, T. R. A. & VECOLI, M. 2012. Systematic occurrences of malformed (teratological) acritarchs in the run-up of Early Palaeozoic δ^{13}C isotope excursions. *Palaeogeography, Palaeoclimatology, Palaeoecology* **367-368**, 137–46.

NANJING INSTITUTE OF GEOLOGY AND MINERAL RESOURCES (ed.) 1983. *Palaeontological Atlas of East China, I. Early Palaeozoic*. Geological Publishing House, Beijing, 657 pp. [in Chinese]

NANJING INSTITUTE OF GEOLOGY AND PALAEONTOLOGY (ed.) 1974. *A handbook of stratigraphy and palaeontology of south-west China*. Science Press, Beijing, 454 pp. [in Chinese]

NICHOLSON, H. A. 1867. On some fossils from the Lower Silurian rocks of the South of Scotland. *Geological Magazine* **1***,* 107–113.

NICHOLSON, H. A. 1868. On the nature and zoological position of the Graptolitidae. *Annals and Magazine of Natural History* **1**, 55–61.

OBUT, A. M., SOBOLEVSKAYA, R. F. & NIKOLAEV, A. A. 1967. *Graptolites and stratigraphy of the lower Silurian along the margins of the Kolyma massif.* Akademiya Nauk SSR, Sibirskoje Otdelenie, Institut Geologii i Geofiziki. Ministerstvo Geologii SSSR, Nauchno-Issledovatel'sky Institut Geologii Arktiki, 164 pp. [in Russian].

PERNER, J. 1895. *Études sur les Graptolites de Bohême. IIième Partie. Monographie des Graptolites de l'Étage D.* Raimond Gerhard, Prague, 31 pp.

PIÇARRA, J. M., ŠTORCH, P., GUTIÉRREZ-MARCO, J. C. & OLIVEIRA, J. T. 1995. Characterization of the *Parakidograptus acuminatus* graptolite Biozone in the Silurian of the Barrancos region (Ossa Morena Zone, south Portugal). *Comunicaçôes do Instituto Geológico e Mineiro* **81**, 3–8.

PIÇARRA, J. M., ROBARDET, M., OLIVEIRA, J. T., PARIS, F. & LARDEUX, H. 2009. Graptolite faunas of the Llandovery "phtanites" at Les Fresnaies (Chalonnes-sur-Loire, southeastern Armorican Massif): Palaeontology and biostratigraphy. *Bulletin of Geosciences* **84**, 41–50.

PODHALAŃSKA, T. 2003. Late Ordovician to Early Silurian transition and the graptolites from Ordovician/Silurian boundary near the SW rim of the East European Craton (Northern Poland). In *Proceedings of the 7th International Graptolite Conference and Field Meeting of the ISSS* (eds G. Ortega, G. & G. F. Aceñolaza), pp. 165–71. *INSUGEO, Serie Correlación Geológica* **18**.

PUDDU, C. & CASAS, J. M. 2011. New insights into the stratigraphy and structure of the Upper Ordovician rocks of the La Cerdanya area (Pyrenees). In *Ordovician of the World* (eds J. C. Gutiérrez-Marco, I. Rábano & D. C. García-Bellido), pp. 441–5. *IGME, Cuadernos del Museo Geominero* **14**.

PUDDU, C., CASAS, J. M. & ÁLVARO, J. J. 2017. On the Upper Ordovician of the La Cerdanya area, Pyrenees. *Géologie de la France* **2017** (1), 26–8.

RICKARDS, R. B. 1970. The Llandovery (Silurian) graptolites of the Howgill Fells, northern England. *Monograph of the Palaeontographical Society* **123** (524), 1–108.

RICKARDS, R. B. & HUTT, J. 1970. The earliest monograptid. *Proceedings of the Geological Society of London* **1663**, 115–9.

ROQUÉ, J. 1999. La Biozona *ascensus–acuminatus* en el Silúrico de las Cadenas Costeras Catalanas (NE de España). *Temas Geológico-Mineros ITGE* **26**, 632–7.

ROQUÉ BERNAL, J., ŠTORCH, P. & GUTIÉRREZ-MARCO, J. C. 2017. Bioestratigrafía (graptolitos) del límite Ordovícico–Silúrico en los Pirineos orientales (curso alto del río Segre, Lleida). *Geogaceta* **61**, 27–30.

ROUSSEL, J. 1904. Tableau stratigraphique des Pyrénées. *Bulletin de la Carte Géologique de la France* **97**, 1–141.

SACHANSKI, V. 1993. Boundaries of the Silurian System in Bulgaria defined by graptolites. *Geologica Balcanica* **23**, 25–33.

SCHAUER, M. 1971. Biostratigraphie und Taxionomie der Graptolithen des tieferen Silurs unter besonderer Berucksichtigung der tektonischen Deformation. *Freiberger Forschungshefte, C**273** Paläontologie*, 1–185.

SCHMIDT, H. 1931. Das Paläozoikum des Spanischen Pyrenäen. *Abhandlungen der Gessellschaft der Wissenschaften zu Göttingen , Mathematik-Physik Klasse 3* [H 5] **8**, 981–1065.

STEIN, V. 1965. Stratigraphische und paläontologische Untersuchungen im Silur des Frankenwaldes. *Neues Jahrbuch für Geologie und Paläontologie, Abhandlungen* **121**, 111–200.

ŠTORCH, P. 1982. Ordovician–Silurian boundary in the northernmost part of the Prague Basin (Barrandian, Bohemia). *Věstník Ústředního ústavu geologického* **57**, 231–6.

ŠTORCH, P. 1983. The genus *Diplograptus* (Graptolithina) from the lower Silurian of Bohemia. *Věstník Ústředního ústavu geologického* **58**, 159–70.

ŠTORCH, P. 1985. *Orthograptus* s.l. and *Cystograptus* (Graptolithina) from the Bohemian lower Silurian. *Věstník Ústředního ústavu geologického* **60**, 87–99.

ŠTORCH, P. 1986. Ordovician–Silurian boundary in the Prague Basin (Barrandian area, Bohemia). *Sborník geologických Věd, Geologie* **41**, 69–103.

ŠTORCH, P. 1992. Some new and little known graptolites from the Lower Silurian of Bohemia (Prague Basin, Barrandian Area). *Časopis pro mineralogii a geologii* **37**, 193–201.

ŠTORCH, P. 1996. The basal Silurian *Akidograptus ascensus–Parakidograptus acuminatus* Biozone in peri-Gondwanan Europe: graptolite assemblages, stratigraphical ranges and palaeobiogeography. *Bulletin of the Czech Geological Survey* **71**, 171–8.

ŠTORCH, P. & FEIST, R. 2008. Lowermost Silurian graptolites of Montagne Noire, France. *Journal of Paleontology* **82**, 938–56.

ŠTORCH, P. & LOYDELL, D. K. 1996. The Hirnantian graptolites *Normalograptus persculptus* and "*Glyptograptus bohemicus*": stratigraphical consequences of their synonymy. *Palaeontology* **39**, 869–81.

ŠTORCH, P. & SCHÖNLAUB, H.-P. 2012. Ordovician–Silurian boundary graptolites of the Southern Alps, Austria. *Bulletin of Geosciences* **87**, 755–66.

ŠTORCH, P. & SERPAGLI, E. 1993. Lower Silurian graptolites from southwestern Sardinia. *Bollettino della Società Paleontologica Italiana* **32**, 3–57.

SUN, Y. C. 1933. Ordovician and Silurian graptolites from China. *Palaeontographica Sinica, B* **14**, 1–52.

TORSVIK, T. H. & COCKS, L. R. M. 2017. *Earth history and palaeogeography*. Cambridge University Press, 317 pp.

TÖRNQUIST, S. L. l897. On the Diplograptidae and Heteroprionidae of the Scanian Rastrites Beds. *Lunds Universitets Årsskrifter* **33**, 1–24.

TRELA, W., PODHAŁAŃSKA, T., SMOLAREK, J. & MARYNOWSKI, L. 2016. Llandovery green/grey and black mudrock facies of the northern Holy Cross Mountains (Poland) and their relation to early Silurian sea-level changes and benthic oxygen level. *Sedimentary Geology* **342**, 66–77.

UNDERWOOD, C. J., CROWLEY, S. F., MARSHALL, J. D. & BRENCHLEY, P. J. 1997. High-resolution carbon isotope stratigraphy of the basal Silurian stratotype (Dob's Linn, Scotland) and its global correlation. *Journal of the Geological Society of London* **154**, 709–18.

UNDERWOOD, C. J., DEYNOUX, M. & GHIENNE, J. F. 1998. High palaeolatitude (Hodh, Mauritania) recovery of graptolite faunas after the Hirnantian (end Ordovician) extinction event. *Palaeogeography, Palaeoclimatology, Palaeoecology* **142**, 91–105.

VANDENBROUCKE, T. R. A., EMSBO, P., MUNNECKE, A., NUNS, N., DUPONCHEL, L., LEPOT, K., QUIJADA, M., PARIS, F., SERVAIS, T. & KIESSLING, W. 2015. Metal-induced malformations in early Palaeozoic plankton are harbingers of mass extinction. *Nature Communications* **6** (7966), 6 pp.

WILLIAMS, M., ZALASIEWICZ, J., BOUKHAMSIN, H. & CESARI, C. 2016. Early Silurian (Llandovery) graptolite assemblages of Saudi Arabia: biozonation, palaeoenvironmental significance and biogeography. *Geological Quarterly* **60**, 3–25.

WILLIAMS, S. H. 1983. The Ordovician-Silurian boundary graptolite fauna of Dob's Linn, southern Scotland. *Palaeontology* **26**, 605–39.

Ye, S. H. 1978. Graptolithina. In *Palaeontological Atlas of Southwest China, Sichuan Volume, Part* 1, *From Sinian to Devonian*, pp. 431–86. Geological Publishing House, Beijing. [in Chinese]
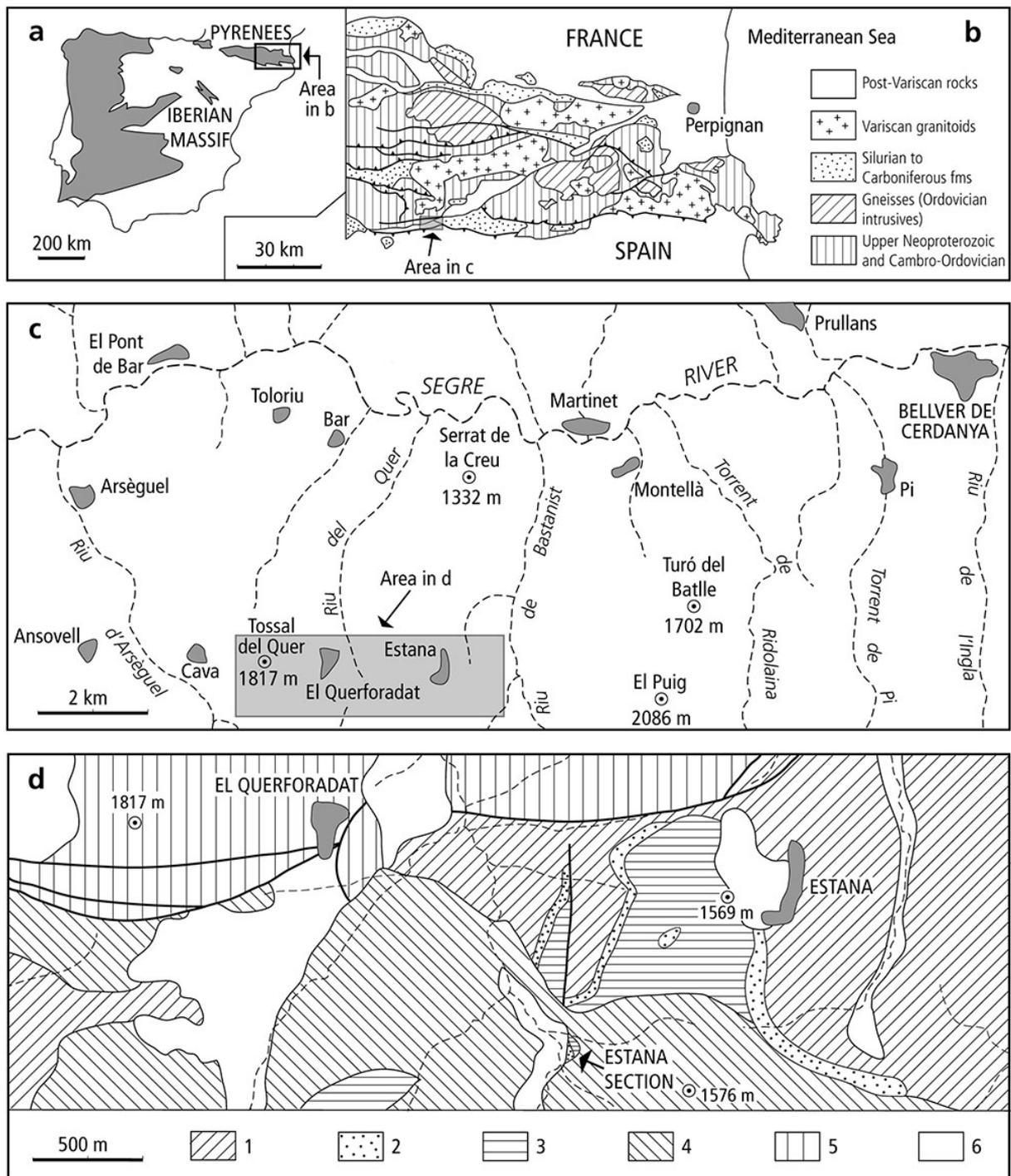
Figure 1. (a) Location map with insets showing Variscan outcrop areas (grey) in the Iberian Peninsula. (b) Geological sketch map of eastern part of the Axial Zone of the Pyrenees. (c) Geographical map of the studied area south of the Segre River valley. (d) Geological sketch map showing position of the Estana section, modified from the Atles Geològic de Catalunya (Institut Geològic de Catalunya and Institut Cartogràfic de Catalunya, 2010): 1, Ansovell Formation, dark shales with interbedded fine-grained sandstones; 2, Bar Formation, grey medium-grained sandstones; 3, black graptolitic shales; 4, dacitic and andesitic lavas of Carboniferous–Permian age; 5, undifferentiated Mesozoic rocks; 6, Quaternary cover.
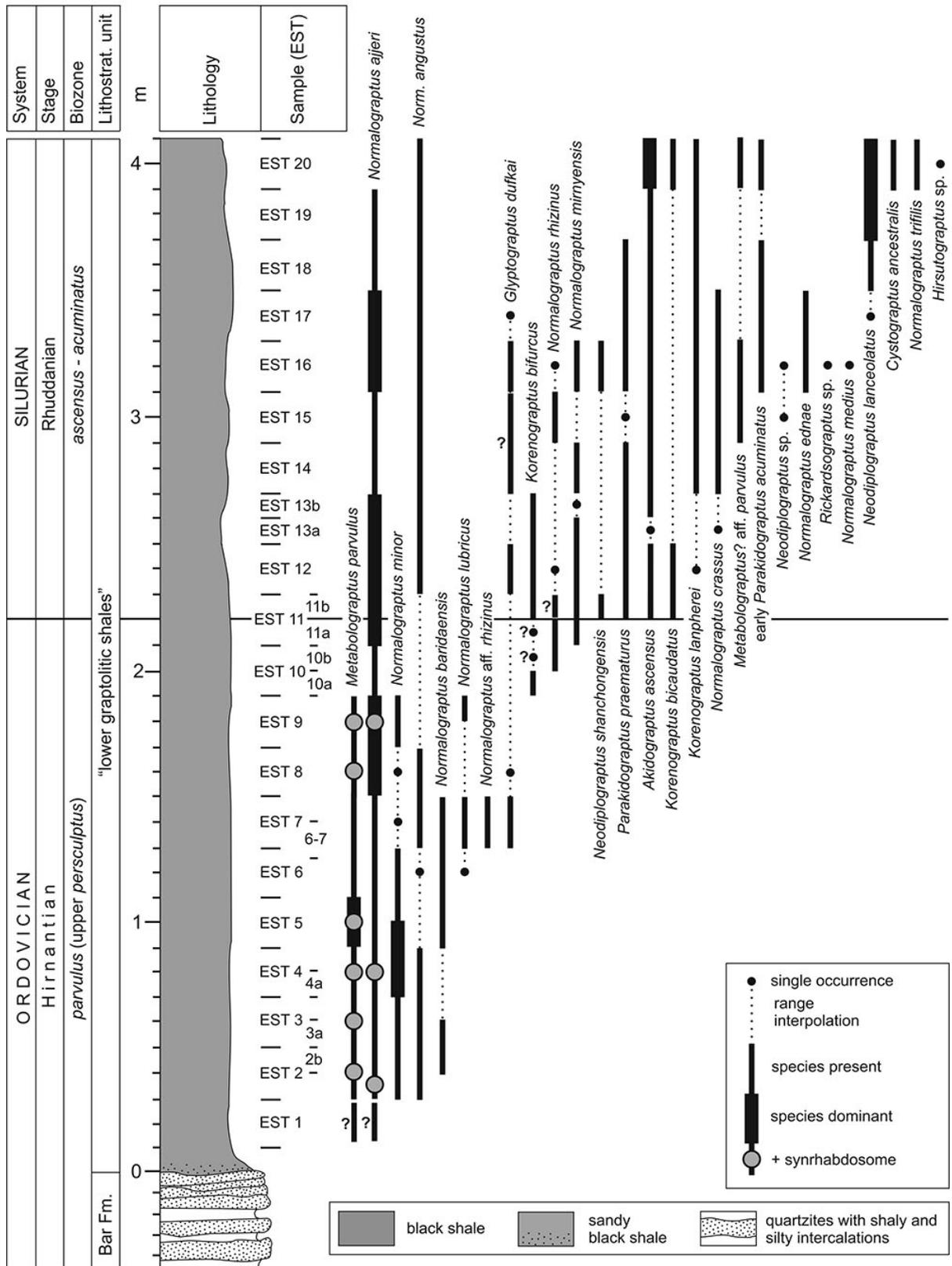
Figure 2. Estana section: lithologies and graptolite fossil record.
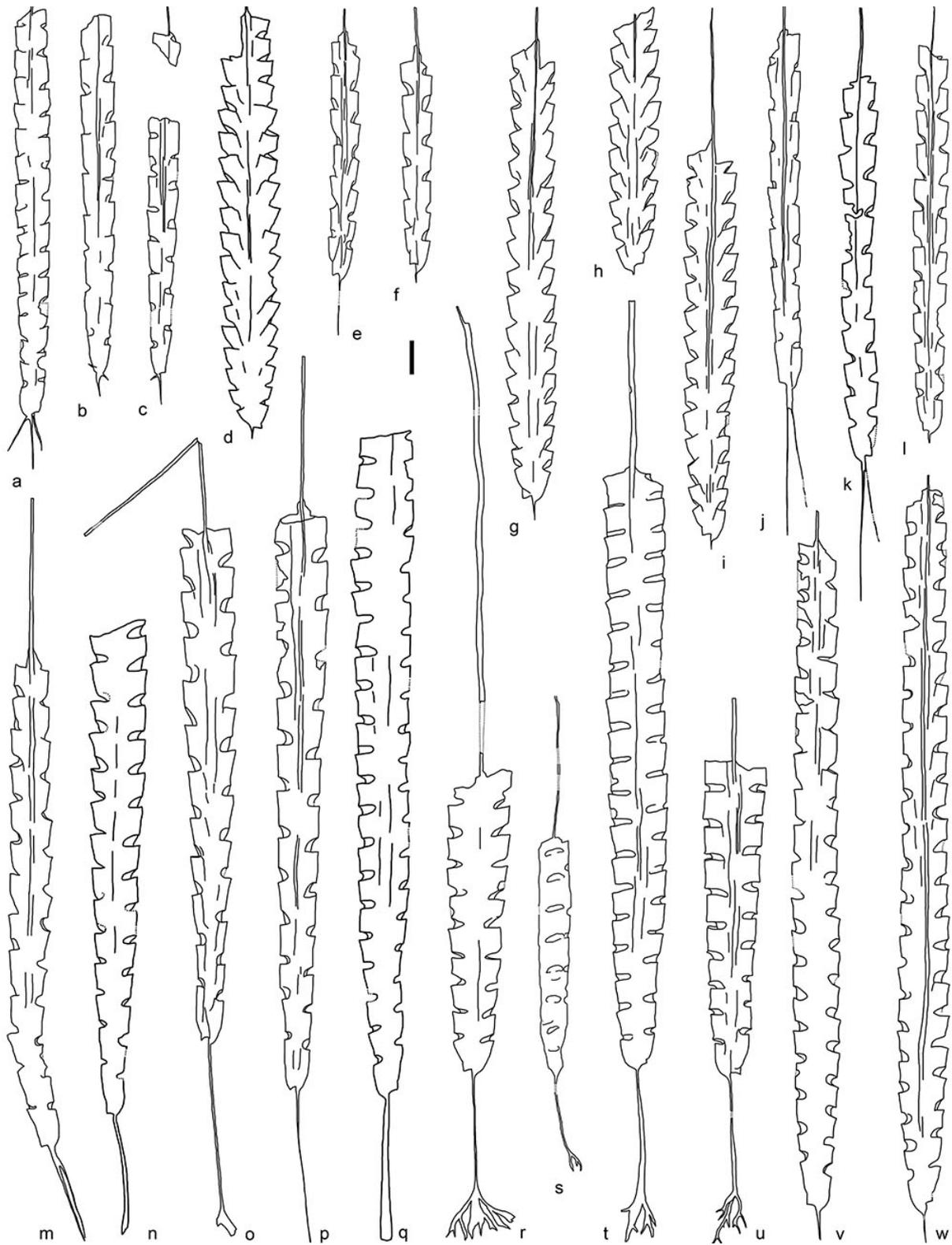
Figure 3. Graptolite fauna of the *parvulus* Biozone. (a–c) *Normalograptus lubricus* (Chen &
Lin, 1978): (a) MGM-8100-O, sample EST 6–7; (b) MGM-8101-O, EST 6–7; (c) MGM-

8102-O, EST 6–7. (d, g–i) *Metabolograptus parvulus* (Lapworth, 1900): (d) MGM-8074-O, EST 4; (g) MGM-8075-O, EST 8; (h) MGM-8076-O, EST 2; (i) MGM-8077-O; EST 7. (e, f, l) *Normalograptus angustus* (Perner, 1895): (e) MGM-8093-O, EST 3a; (f) MGM-8094-O, EST 7; (l) MGM-8095-O, EST 8. (j, k, m) *Normalograptus baridaensis* sp. nov.: (j) holotype, MGM-8096-O, EST 2b; (k) MGM-8099-O, EST 2b–3a; (m) MGM-8098-O, EST 2b. (n, q) *Normalograptus rhizinus* (Li & Yang, 1983): (n) MGM-8106-O, EST 10b; (q) MGM-8107-O, EST 10b. (o, p) *Normalograptus* aff. *rhizinus* (Li & Yang, 1983): (o) MGM-8104-O, EST 7; (p) MGM-8105-O, EST 7. (r–u) *Normalograptus minor* (Huang, 1982): (r) MGM-8088-O, EST 3; (s) MGM-8089-O, EST 7; (t) MGM-8091-O, EST 4a; (u) MGM-8090-O, EST 5. (v, w) *Normalograptus ajjeri* (Legrand, 1977): (v) MGM-8082-O, EST 7; (w) MGM-8083-O, EST 9. All specimens x 6, black bar represents 1 mm.
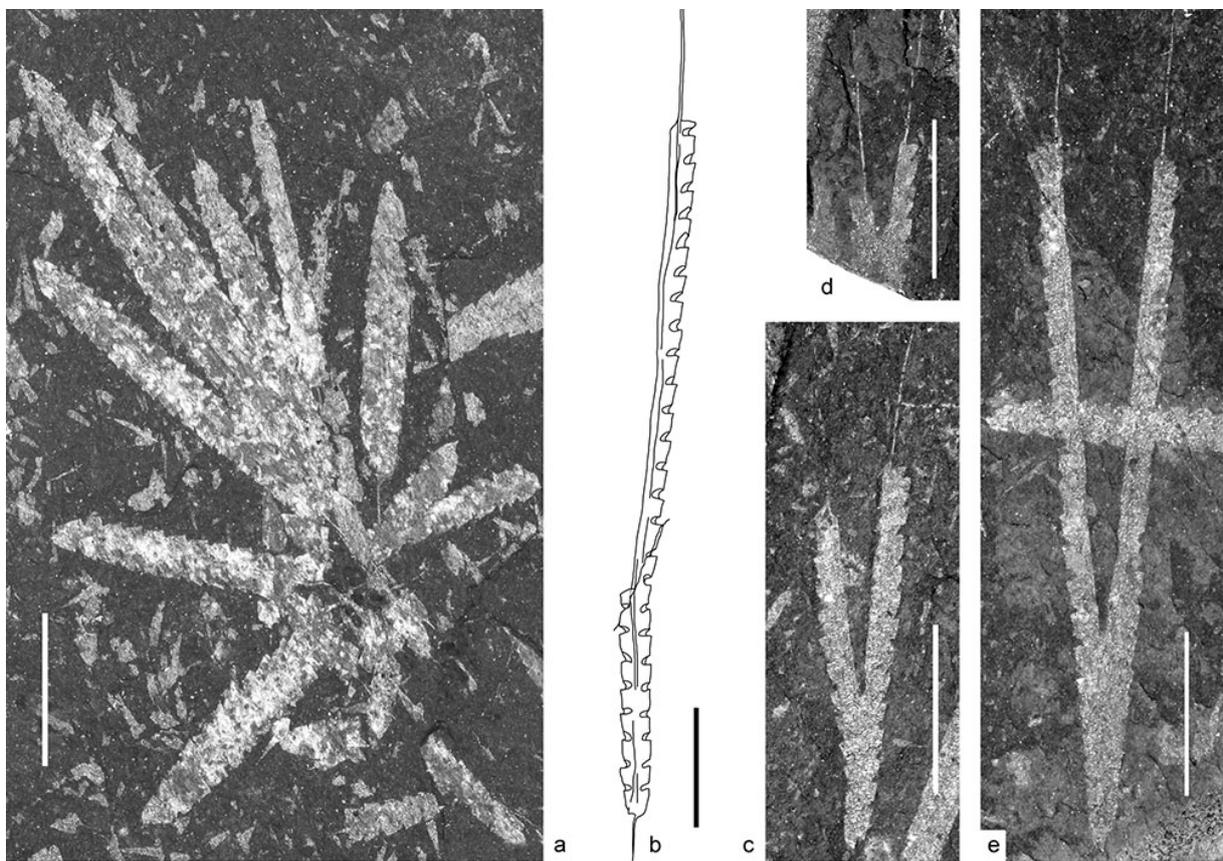
Figure 4. (a) Radially arrayed synrhabdosome of *M. parvulus* (Lapworth, 1900), MGM-8081-O, sample EST 3. (b) *Normalograptus ajjeri* (Legrand, 1977) with long uniserial portion, MGM-8084-O, EST 8–9 (1.6–1.8 m above the top of the Bar Formation). (c–e) Abnormal normalograptid rhabdosomes distally forked into two uniserial stipes: (c) MGM-8085-O, EST 8–9; (d) MGM-8086-O, EST 8–9; (e) MGM-8087-O, EST 8–9. Black and white scale bars represent 5 mm.
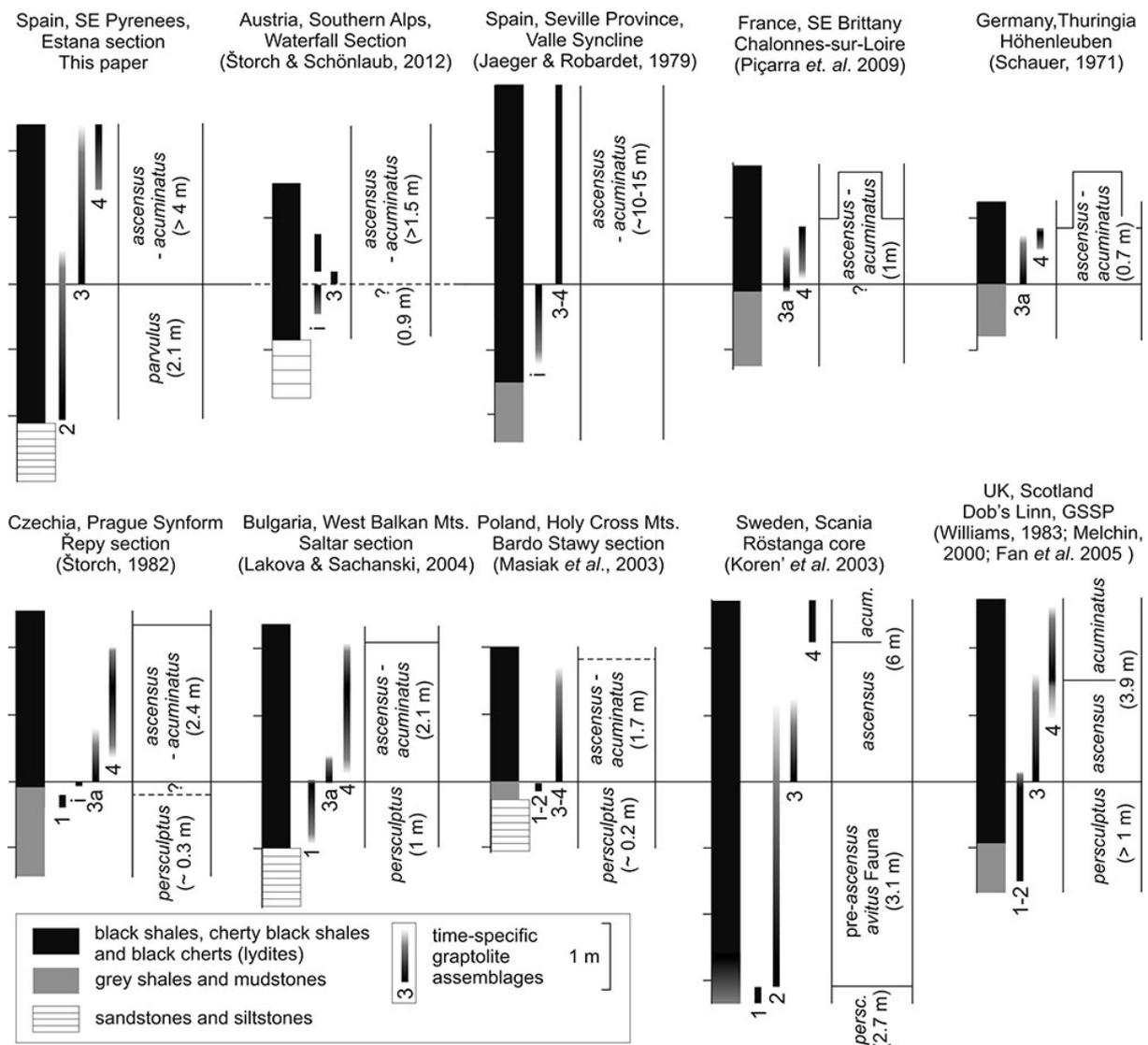
Figure 5. Correlation of the most complete graptolite-bearing Ordovician–Silurian boundary sections of Europe. Time-specific graptolite assemblages discussed in this paper: 1 – upper Hirnantian fauna including *M. persculptus*; 2 – graptolite assemblage of the *parvulus* (upper *persculptus*) Biozone – lowermost *ascensus–acuminatus* Biozone characterized by *M. parvulus*, *N. minor*, *N. rhizinus* and *Nd. shanchongensis* which are accompanied either by *N. avitus* s.s., *N. avitus* of Williams, 1983 and *K. laciniosus* in low latitude sections (*avitus* Fauna of Koren' *et al.* 2003), or by *N. lubricus* and *K. bifurcus* in the peri-Gondwanan realm; 3 – graptolite assemblage of the lowermost *ascensus–acuminatus* Biozone marked by the appearance of *A. ascensus* and *Par. praematurus* in association with either taxa inherited from the previous assemblage or with *Nd. lanceolatus* (Assemblage 3a); 4 – classical assemblage of the lower-middle *ascensus–acuminatus* Biozone characterized by the co-occurrence of *A. ascensus* and *Par. acuminatus* along with *Nd. lanceolatus*, *N. trifilis* and *Cyst. ancestralis*; i – graptolite assemblage limited to indeterminable or long-ranging normalograptids.
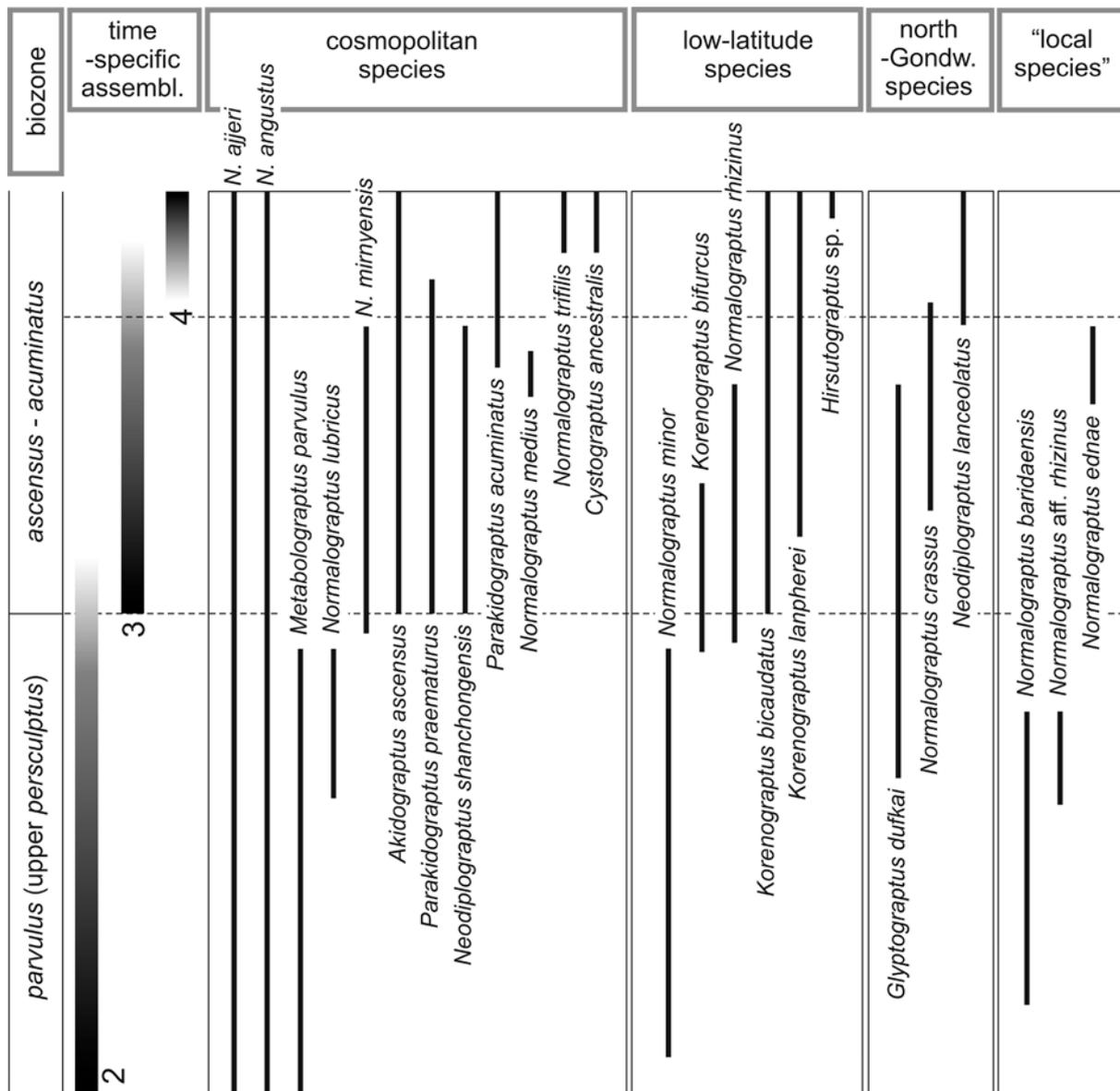
32

Figure 6. Time-specific graptolite assemblages of the *parvulus* (upper *persculptus*) and lower–middle *ascensus–acuminatus* biozones recognized in the Estana section. The species are grouped according to their palaeogeographical distribution: Cosmopolitan species, species previously known only from low-latitude palaeoplates, species confined in peri-Gondwanan Europe (i.e. north-western peri-Gondwana), and 'local species' recorded solely in the Estana Section.
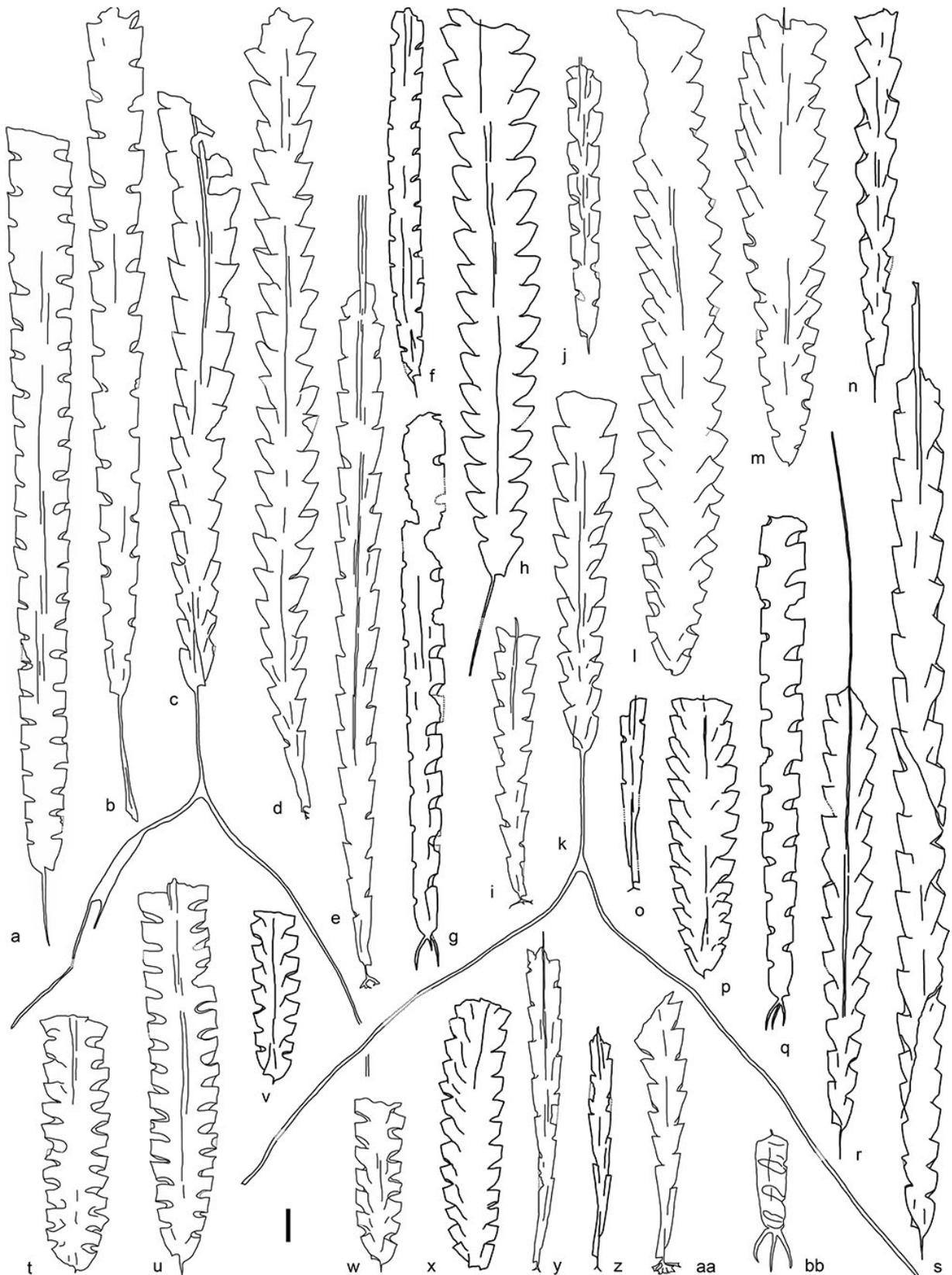
Figure 7. Graptolite fauna of the *ascensus–acuminatus* Biozone. (a) *Normalograptus ajjeri* (Legrand, 1977): MGM-1703-S, sample EST 13b. (b) *Normalograptus rhizinus* (Li & Yang, 1983): MGM-1719-S, EST 16. (c, k) *Korenograptus bifurcus* (Mu *et al.*, 1974): (c) MGM-

1714-S, EST 12; (k) MGM-1715-S, EST 12. (d, aa) *Parakidograptus acuminatus* (Nicholson, 1867), early form: (d) MGM-1756-S, EST 20; (aa) MGM-1757-S, EST 16. (e, i) *Parakidograptus praematurus* (Davies, 1929): (e) MGM-1730-S, EST 13a; (i) MGM-1731-S, EST 13a. (f) *Normalograptus mirnyensis* (Obut & Sobolevskaya, 1967): MGM-1721-S, EST 16. (g, q, bb) *Normalograptus ednae* sp. nov.: (g) MGM-1760-S, EST 16; (q) holotype, MGM-1761-S, EST 16; (bb) MGM-1762-S, EST 16. (h) *Korenograptus lanpherei* (Churkin & Carter, 1970): MGM-1749-S, EST 16. (j) *Normalograptus angustus* (Perner, 1895): MGM-1708-S, EST 13b. (l, m) *Neodiplograptus lanceolatus* Štorch & Serpagli, 1993: (l) MGM-1773-S, EST 19; (m) MGM-1774-S, EST 19. (n, r, s) *Glyptograptus dufkai* Štorch, 1992: (n) MGM-1709-S, EST 16; (r) MGM-1710-S, EST 16; (s) MGM-1711-S, EST 12. (o, y, z) *Akidograptus ascensus* Davies, 1929: (o) MGM-1738-S, EST 16; (y) MGM-1739-S, EST 15; (z) MGM-1740-S, EST 16. (p, x) *Neodiplograptus shanchongensis* (Li, 1984): (p) MGM-1722-S, EST 16; (x) MGM-1723-S, EST 16. (t, u) *Normalograptus crassus* Štorch & Feist, 2008: (t) MGM-1754-S, EST 15; (u) MGM-1755-S, EST 14. (v, w) *Neodiplograptus* sp.: (v) MGM-1758-S, EST 16; (w) MGM-1759-S, EST 15. All specimens x 6, black bar represents 1 mm.
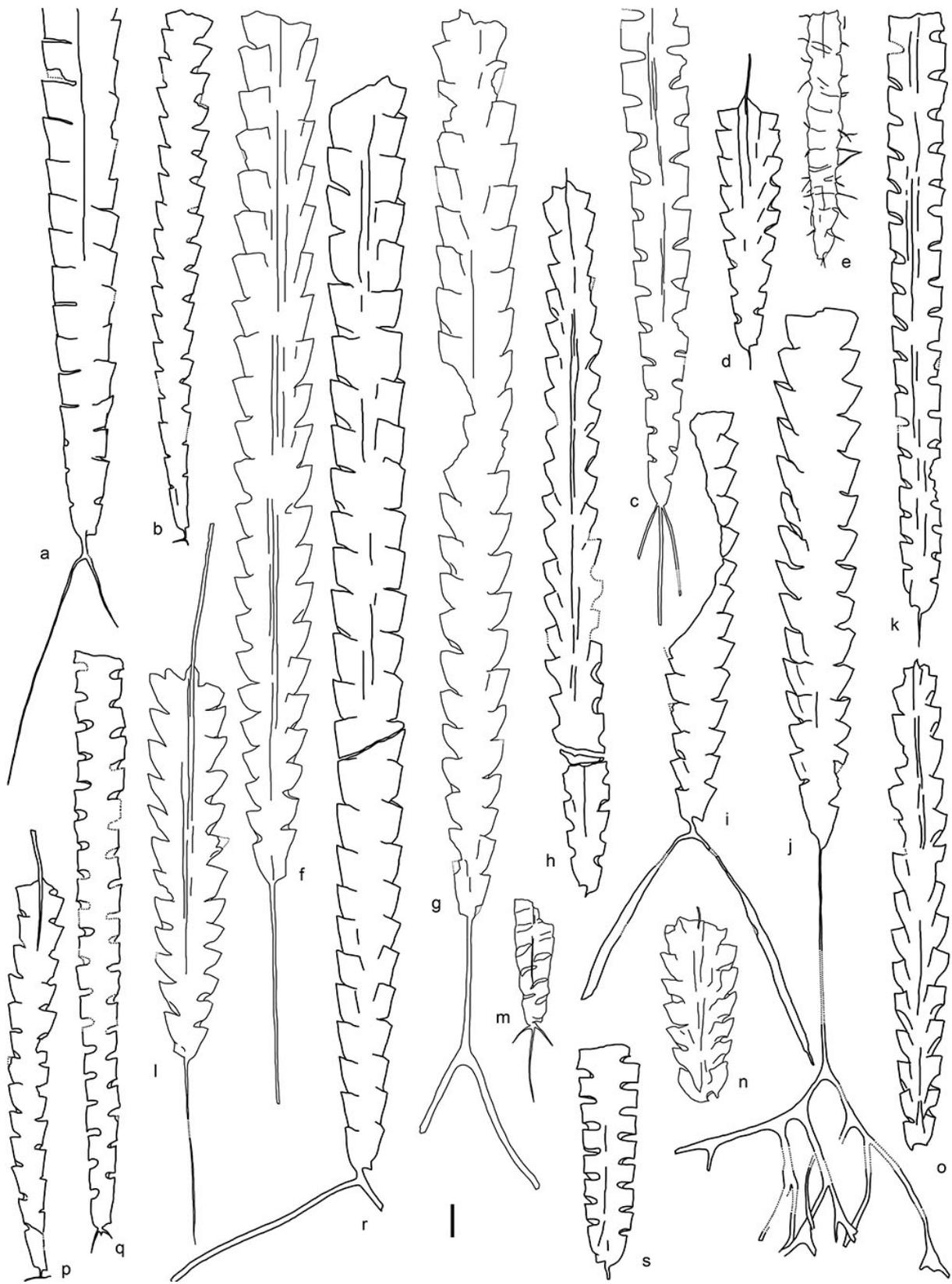
Figure 8. Graptolite fauna of the *ascensus–acuminatus* Biozone, continued. (a, ?i, r) *Korenograptus bicaudatus* (Chen & Lin, 1978): (a) proximal part of 52 mm long specimen,

MGM-1745-S, sample EST 12; (?i) rhabdosome in profile with slightly arcuate branches of the bifurcated virgella, MGM-1746-S, EST 12; (r) MGM-1747-S, EST 12. (b, p) *Parakidograptus praematurus* (Davies, 1929): (b) MGM-1732-S, EST 11b; (p) MGM-1733-S, EST 11b. (c, m) *Normalograptus trifilis* (Manck, 1923): (c) MGM-1781-S, EST 20; (m) MGM-1782-S, EST 20. (d) *Rickardsograptus* sp.: MGM-1771-S, EST 16. (e) *Hirsutograptus* sp.: MGM-1786-S, EST 20. (f, l) *Korenograptus lanpherei* (Churkin & Carter, 1970): (f) MGM-1750-S, EST 14; (l) MGM-1751-S, EST 12. (g, ?j) *Korenograptus bifurcus* (Mu *et al.*, 1974): (g) MGM-1716-S, EST 13a; (?j) MGM-1717-S, EST 12. (h, o) *Metabolograptus*? aff. *parvulus* (Lapworth, 1900): (h) MGM-1767-S, EST 16; (o) MGM-1768-S, EST 16. (k) *Normalograptus ajjeri* (Legrand, 1977): MGM-1704-S, EST 11b. (n) *Cystograptus ancestralis* Štorch, 1985: MGM-1778-S, EST 20. (q) *Normalograptus ednae* sp. nov.: MGM-1763-S, EST 16. (s) *Normalograptus medius* (Törnquist, 1897): MGM-1772-S, EST 16. All specimens x 6, black bar represents 1 mm.
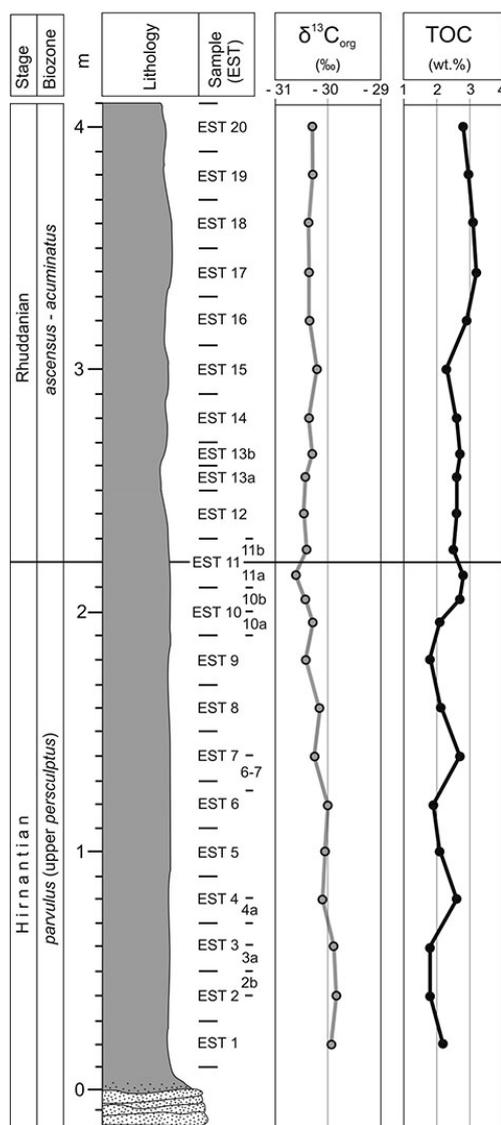

Figure 9. $\delta^{13}C_{org}$ isotopic record in the Estana section plotted with TOC. See Figure 2 for lithology explanations and abbreviations.
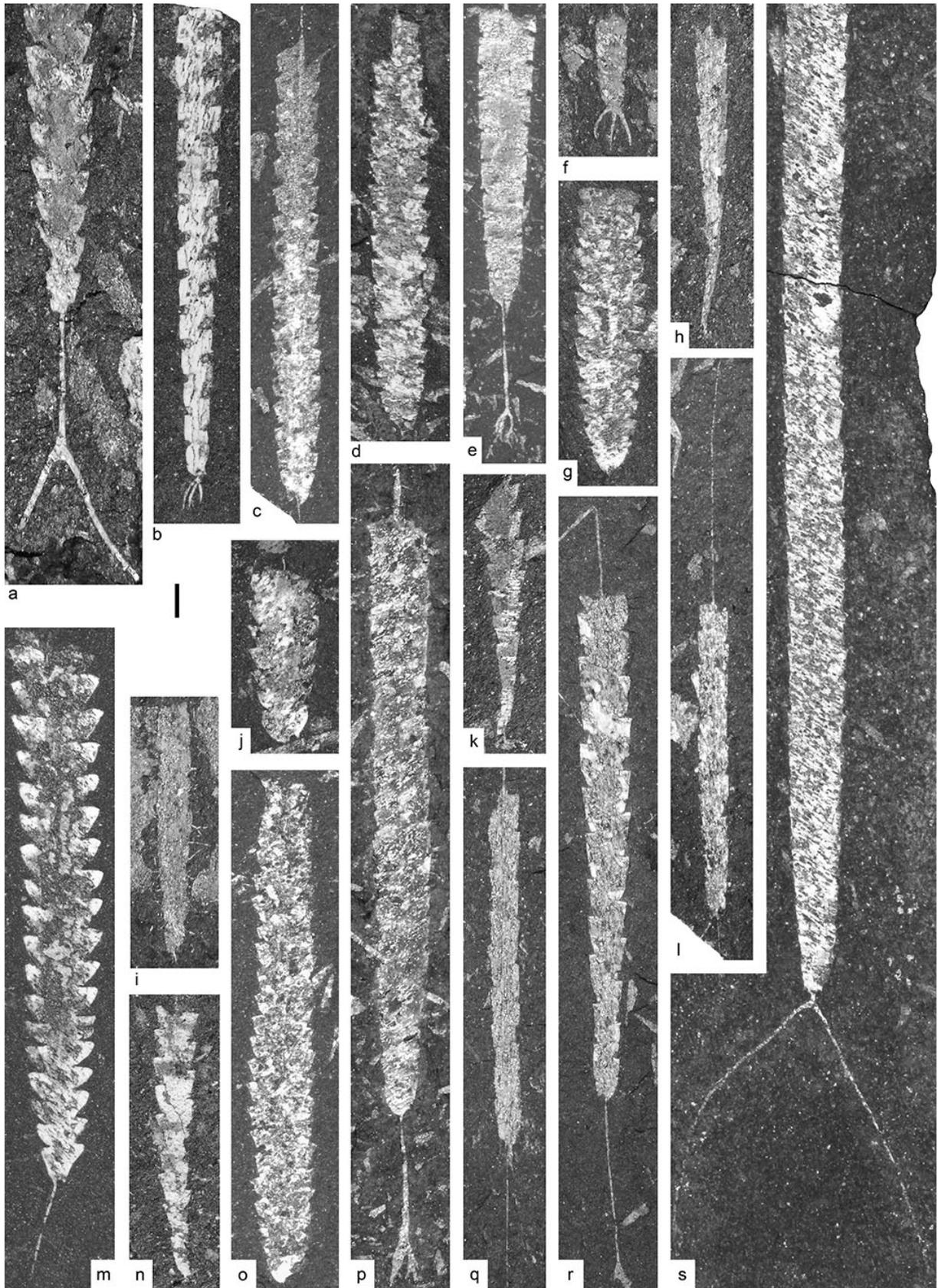
Figure 10. (a) *Korenograptus bifurcus* (Mu *et al.*, 1974): MGM-1716-S, sample EST 13a. (b, f) *Normalograptus ednae* sp. nov.: (b) holotype, MGM-1761-S, EST 16; (f) MGM-1762-S, EST 16. (c, d) *Metabolograptus parvulus* (Lapworth, 1900): (c) MGM-8075-O, EST 8; (d)

MGM-8074-O, EST 4. (e, p) *Normalograptus minor* (Huang, 1982): (e) MGM-8090-O, EST 5; (p) MGM-8091-O, EST 4a. (g, o) *Neodiplograptus shanchongensis* (Li, 1984): (g) MGM-1722-S, EST 16; (o) MGM-1724-S, EST 11b. (h) *Akidograptus ascensus* Davies, 1929: MGM-1739-S, EST 15. (i) *Hirsutograptus* sp.: MGM-1786-S, EST 20. (j) *Cystograptus ancestralis* Štorch, 1985: MGM-1778-S, EST 20. (k) *Parakidograptus acuminatus* (Nicholson, 1867), early form: MGM-1757-S, EST 16. (?l, q) *Normalograptus baridaensis* sp. nov.: (?l) MGM-8097-O, EST 6; (q) holotype, MGM-8096-O, EST 2b. (m) *Korenograptus lanpherei* (Churkin & Carter, 1970): MGM-1749-S, EST 16. (n) *Parakidograptus praematurus* (Davies, 1929): MGM-1731-S, EST 13a. (r) *Normalograptus* aff. *rhizinus* (Li & Yang, 1983): MGM-8104-O, EST 7. (s) *Korenograptus bicaudatus* (Chen & Lin, 1978): MGM-1748-S, EST 12. All specimens x 6, black bar represents 1 mm.